REPORT DOCUMENTATION PAGE

AFOSR-TR-95

0605

1. AGENCY USE ONLY (Leave blank)	2. REPORT DATE	3. REPORT TYPE AND DATES COVERED
	9/14/95	Final Technical Report 7/15/92-7/31/95

4. TITLE AND SUBTITLE

Selective Processing Techniques For Electronic And Opto-Electronic Applications: Quantum-Well Devices And Integrated Optic Circuits

5. FUNDING NUMBERS

~~F49620-92-J-0414~~
61102F
2301/AS

6. AUTHOR(S)

Richard M. Osgood, Jr.

7. PERFORMING ORGANIZATION NAME(S) AND ADDRESS(ES)

Columbia University
Microelectronics Sciences Laboratories
500 West 120th Street
1001 Schapiro CEPSR
New York, New York 10027

8. PERFORMING ORGANIZATION REPORT NUMBER

9. SPONSORING/MONITORING AGENCY NAME(S) AND ADDRESS(ES)

Air Force Office of Scientific Research - NE
Building 410
Bolling AFB, DC 20332-6448

10. SPONSORING/MONITORING AGENCY REPORT NUMBER

F49620-92-J-0414

11. SUPPLEMENTARY NOTES

The view, opinions and/or findings contained in this report are those of the author(s) and should not be construed as an official Department of the position, policy, or decision, unless so designated by other documentation.

12a. DISTRIBUTION/AVAILABILITY STATEMENT

Approved for public release; distribution unlimited.

12b. DISTRIBUTION CODE

13. ABSTRACT (Maximum 200 words)

The goal of this DARPA/AFOSR program was to apply selective processing techniques developed at Columbia to the fabrication of specific device structures for both integrated optical and microelectronic devices and systems. Two technology areas were addressed: a) new techniques appropriate for processing sensitive MQW devices, and b) fabrication of integrated optical devices and circuits. A key aspect of this work has been collaborations with other industrial and university partners.

19951004 134

DTIC QUALITY INSPECTED 5

14. SUBJECT TERMS	15. NUMBER OF PAGES
channel dropping filter, thin-film isolator, via etching laser wet etching, MQWs	50
	16. PRICE CODE

17. SECURITY CLASSIFICATION OF REPORT	18. SECURITY CLASSIFICATION	19. SECURITY CLASSIFICATION OF ABSTRACT	20. LIMITATION OF ABSTRACT
UNCLASSIFIED	UNCLASSIFIED	UNCLASSIFIED	UL

SELECTIVE PROCESSING TECHNIQUES FOR ELECTRONIC AND OPTO-ELECTRONIC APPLICATIONS: QUANTUM-WELL DEVICES AND INTEGRATED OPTIC CIRCUITS

Principal Investigator: Richard M. Osgood, Jr.

Columbia University
Microelectronics Sciences Laboratories
500 West 120th Street
1001 Schapiro CEPSR
New York, NY 10027

Final Technical Report for the Period
July 15, 1992 - July 31, 1995

Submitted: September 14, 1995

Prepared For
USAF, AFSC
Air Force Office of Scientific Research
Building 410
Bolling AFB, DC 20332-6448

Sponsored by
Advanced Research Projects Agency (ARPA)
ARPA Order No. 6321
Monitored by the Air Force Office of Scientific Research under Contract #F49620-92-J-0414

Table of Contents

Introduction

The goal of this DARPA/AFOSR program was to apply selective processing techniques developed at Columbia to the fabrication of specific device structures for both integrated optical and microelectronic devices and systems. Two technology areas were addressed: a) new techniques appropriate for processing sensitive MQW devices, and b) fabrication of integrated optical devices and circuits. A key aspect of this work has been collaborations with other industrial and university partners. Our industrial partners have included Ray Wolfe at AT&T, Paul Lin at Bellcore, Frank Tong at IBM, Jim Yardley at Allied Signal, and Bill Hooper at Hughes Research Laboratories.

The report is organized so as to address the following research areas: Processing for Integrated Optical Devices and Technology, Writing Technology, and Processing for Ultra Devices.

I. Processing for Integrated Optical Devices and Technology

A. Channel Dropping Filter

In the previous DARPA/AFOSR program, we succeeded in developing a direct-etch fabrication technology suitable for rapid prototyping of passive and active integrated optical device structures. In this program we applied these techniques to the fabrication of new and complex devices, such as the narrow-band channel-dropping filter (CDF) proposed by H.A. Haus at M.I.T., and end-facet grating based multiplexers. [Other components fabricated using rapid prototyping are described in Section III below.]

A channel dropping filter has been fabricated and tested, and was found to exhibit the basic behavior predicted from the theory, including a sub-Angstrom bandwidth. This is the first experimental realization of this important telecommunications device first proposed by H.A. Haus

at M.I.T. The very first devices showed promise, but required redesign.

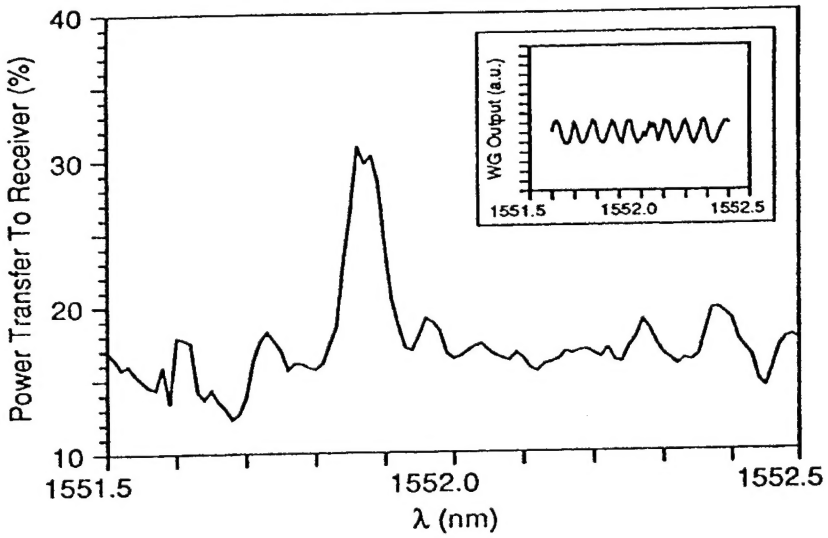

Fig. 1. Response of narrow-band channel dropping filter. The bandwith is 0.8Å FWHM.

We analyzed the devices using a recently introduced tunable laser source from HP. A portion of the response is shown in Fig. 1, which shows the output of the resonator arm versus wavelength. A strong resonant peak is observed, which corresponds to the predicted transmission resonances. The power transfer of 30% approaches the theoretical maximum of 50% for this design. Finally, the bandwidth is 0.8Å FWHM, within the predicted sub-Angstrom range, and the narrowest value of any integrated filter design. This is the first demonstration of a CDF of this type, and represents an important step in the development of this technology area. A paper on this work was published in Photonics Technology Letters.

Initial tests of the device exhibited high-frequency Fabry-Perot oscillations superimposed on the main response of the device. To reduce these oscillations we coated the facets of the device with an anti-reflection coating. The AR-coating was performed by Nicholas Andreadakis of Bellcore, Red Bank. The measured response of the CDF, shown in Fig. 2, demonstrates that the high-

frequency ringing was eliminated.

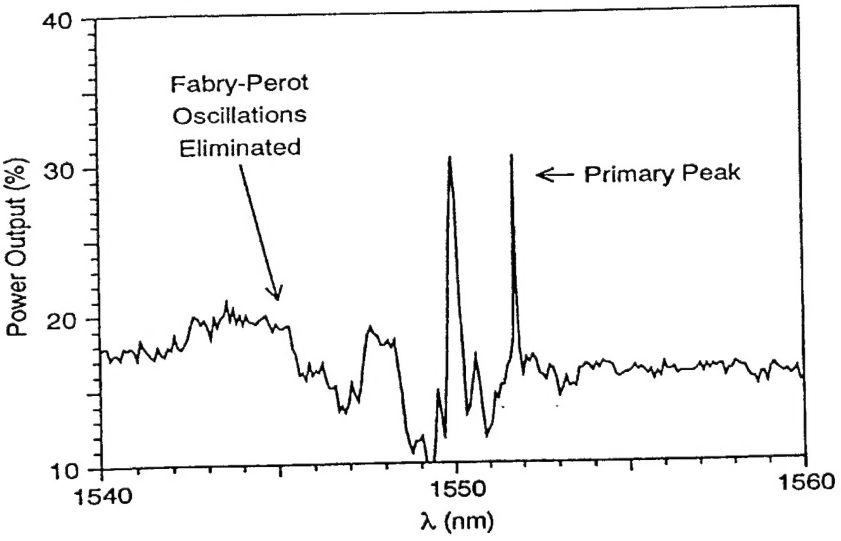

Fig. 2. Response of CDF with antireflection coatings to eliminate Fabry-Perot oscillations.

Also during this period we performed temperature tuning tests on the filters and observed a tunability of 1 Å/°C on the peak position of the resonant response. This is shown in Fig. 3. This tunability can be extremely useful in multiwavelength networking applications, in which a receiver circuit might be built using one CDF instead of several, thus reducing costs.

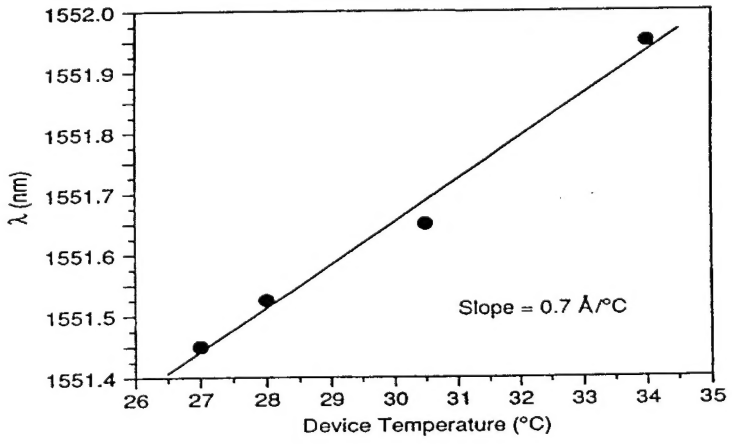

Fig. 3. Temperature dependence of CDF center wavelength.

There are several characteristics of our initial design which need to be addressed before it can be considered for realistic application to networking and other areas. Thus we have recently fabricated a second generation of channel-dropping filters which incorporate improvements in design based on the analysis of the performance of the original device. The first issue is the presence of a second peak in the spectral response and the second is a significant amount of background superimposed on the signal. Extensive computer modelling described below showed that these features could be traced to the presence of additional waveguide modes in the coupling region, not in the individual waveguides which we had guarded against. The theoretical response we obtained is shown in Fig. 4. Armed with this analysis, we went back and redesigned the coupler to reduce or eliminate the presence of higher order coupler modes; it is the improved version which we have fabricated this year and are about to test.

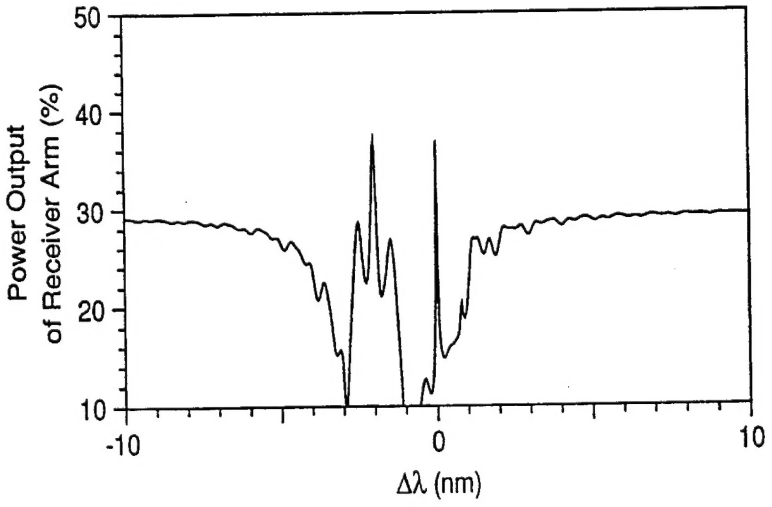

Fig. 4. Theoretical response of multimode CDF.

Fabrication of the new CDF called for improvements in direct laser-writing technology, which we utilize to pattern these devices. In particular, we found that the narrower coupling region,

required to eliminate spurious waveguide modes, had a significantly detrimental effect on the coupling efficiency of the device. Software modifications to the existing laser-write code were needed to increase our patterning resolution, which would otherwise lead to a significant reduction in the output intensity of the filtered narrow-band signal. Figure 5 illustrates the improvements in direct-write patterning resolution on the response of the coupler. Fabrication of the resonator grating for these devices was done by Paul Lin, of Bellcore, Red Bank. These latest results were presented at the Annual Meeting of the Optical Society of America in October, 1994.

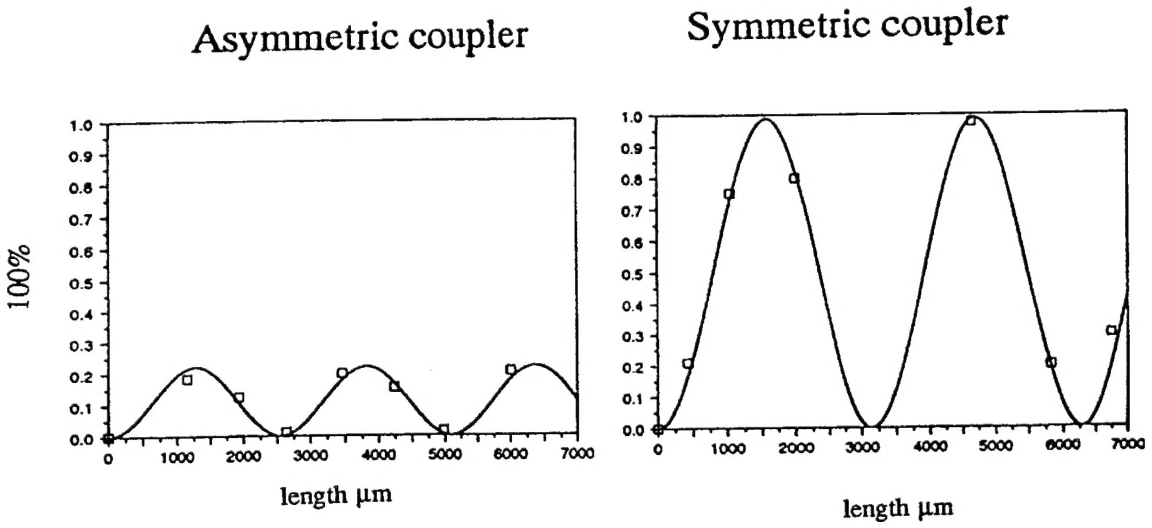

Fig. 5: Comparison of response times for symmetric and asymmetric couplers. Note that careful software adjustment of stage motion parameters improves resolution.

B. Thin-Film Isolator

Integrated optical isolators are an extremely important and thus far unavailable component for integrated optical systems; we have made significant accomplishments in realizing such devices during this period. Our eventual goal is to obtain a magneto-optic isolator driven by thin-film magnets, which could be integrated directly onto optical chips. Detailed calculations of the magnetic

fields produced by recently developed magnetic thin-films showed that saturation of properly designed Bi-YIG materials might be achieved.

The work involved collaboration with R. Wolfe at Bell Labs who provided the Bi-YIG waveguide, and C.J. Gutierrez and G.A. Prinz at NRL who provided thin-film magnets to realize our design. Fabrication and testing of the final device was done by our group at Columbia. Measurements indicate that the thin-film magnets can nearly saturate the Bi-YIG. In addition, the device exhibited good isolation behavior as shown in Fig. 6, which displays the optical output through the Bi-YIG waveguides for two different orientations of the magnetic thin-film. The isolation ratio obtained was 21 dB. The initial device used a 1.5μm Fe-Co film as magnet on the Bi-YiG waveguide base. This result represents the first demonstration of a thin-film magnet magneto-optic isolator. This has been published and appeared Photonics Technology Letters.

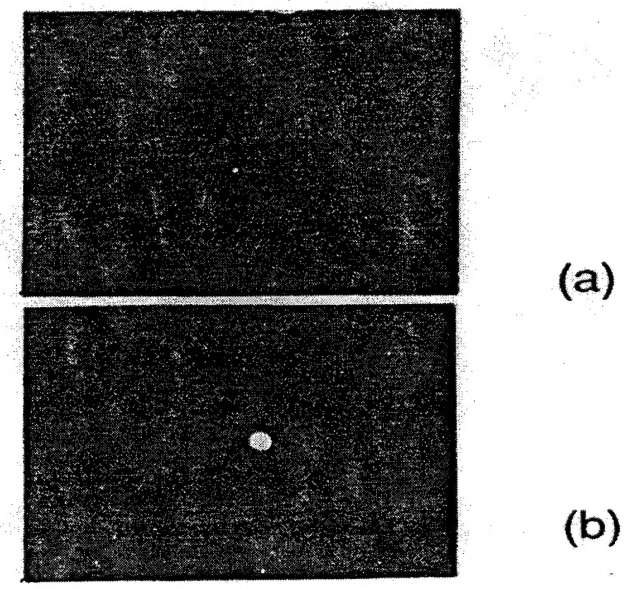

Fig. 6. Output of thin-film-magnet magneto-optic isolator for two different film orientations.

Subsequently, we improved the performance of the device by using a thicker magnet to provide full saturation of the magnetization in the isolator waveguide. The magnet used was a high-coercivity sputtered samarium-cobalt film magnet fabricated by Fred Cadieu of Queens College. This is a 22μm-thick polycrystalline film with a coercivity larger than 1 KOe, and is therefore a better permanent magnet than the Fe-Co single crystals used in our initial tests of the isolator. It also produces a larger net effective field because of its larger thickness. Using these magnets we have obtained ratios of about 25 dB in the range of wavelengths between 1549 and 1560 nm, and a forward loss of less than 1 dB throughout the whole range. This is plotted in Figs. 7 and 8. The improved performance of the isolator is due to full saturation of the magnetization by the more powerful Sm-Co film and to an improved launching technique to overcome the deleterious effects of birefringence.

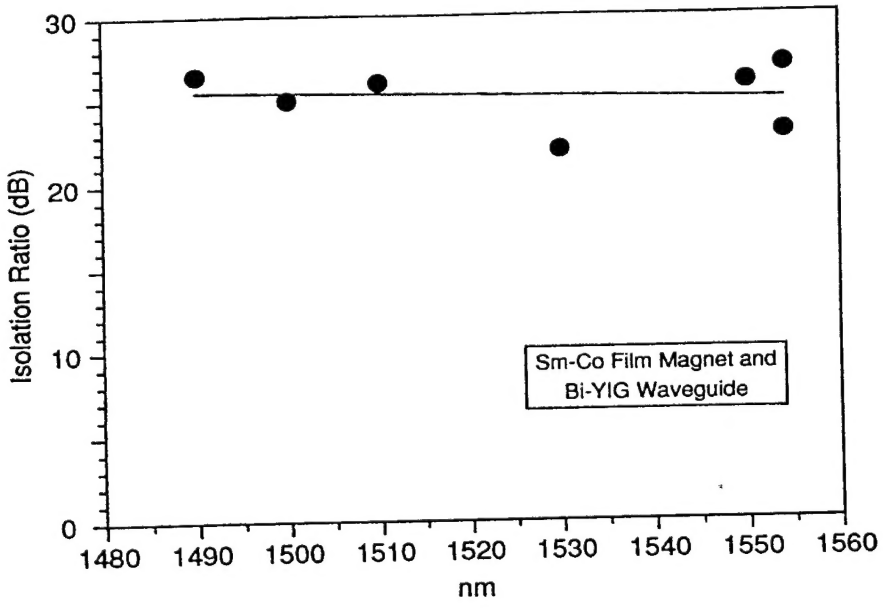

Fig. 7. Isolation ratio versus wavelength for thin-film isolator.

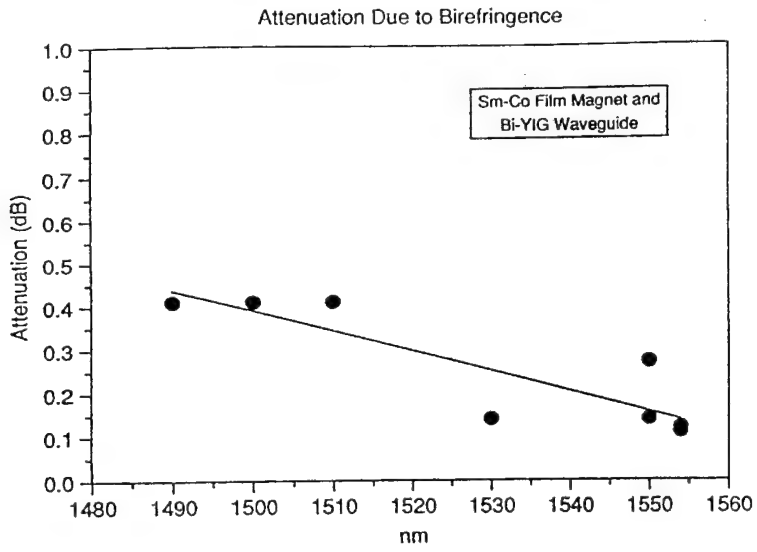

Fig. 8. Attenuation versus wavelength for thin-film isolator.

These results were presented at the Magnetism and Magnetic Materials Conference in Minneapolis, November, 1993 and have been subsequently published.

C. Applications of Through-Wafer Via Etching

In the previous contract, we reported the development of a technique for rapid etching of through-wafer vias in SI-InP. In collaboration with Hughes, we had applied the technique to the fabrication of vias in actual MMIC microwave devices. This work has now been published in the IEEE Transactions on Semiconductor Manufacturing.

In the first year of this contract, we successfully transferred this technology to Hughes, where they then replicated our experimental setup in their labs. In addition, we have fabricated additional devices for microwave testing.

Finally, we have investigated a new application which uses our via etching process to fabricate large arrays of cylindrical vias which can act as transmission filters in the infrared. The

filter consists of a series of cylindrical waveguides that are ~ 20 μm in diameter and ~ 100 μm in depth, with smooth straight sidewalls. The side walls must be highly conductive to avoid penetration of the waveguide mode into the walls.

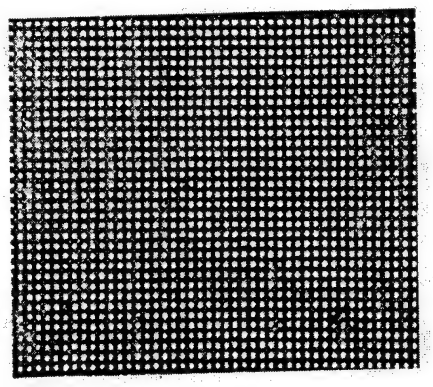

Figure 9. Optical photograph of an array of vias etched in SI-InP for use as an IR transmission filter.

The filter is formed from a 100μm thick SI-InP Fe-doped substrate. The pattern consists of a grid with ~ 20 μm laser etched through via holes, with 50 μm center-to-center spacing, as shown in Fig. 9. The entire pattern covers an area of 3 mm x 3 mm. The sample is mounted vertically in a quartz cell on a computer controlled X,Y,Z stage with an opening on the back. The opening allows the laser light to penetrate through the wafer onto a photodetector. This detector sends a voltage signal to the computer to shut off the beam, move to the next via location, and open the shutter to drill the next via. Thus the opening served as an end-point detection. With this arrangement, the holes obtained were very uniform in diameter and etch time. The average via etch time was ~ 10 seconds. After the etching, the sample was removed and rinsed in deionized water leaving the deeply etched through-holes clear as shown in Fig. 9. The sample was then metallized Cr and Al, using e-beam and thermal evaporation, respectively. The chromium and aluminum layers which covered the walls of the vias were ~ 200 Å and 7000 Å, respectively, resulting in highly conductive cylindrical waveguides.

The far-infrared transmission spectrum of this waveguide filter was measured using a Perkin Elmer spectrometer at $2cm^{-1}$ resolution. A globar was used as the source and a DTGS bolometer as detector. Figure 10 shows the plot of the transmittance vs. wavenumbers. The position of the cutoff is at 242.2 cm^{-1} which corresponds to a cutoff wavelength of ~ 41 μm. The theory predicts that the cutoff wavelength is twice the diameter of the via hole. In our case the average diameter of the via is ~ 21 μm, implying a cutoff of 42 μm, in good agreement with the measurement. As shown in Fig. 10, the cutoff is very steep giving the filter a very high contrast.

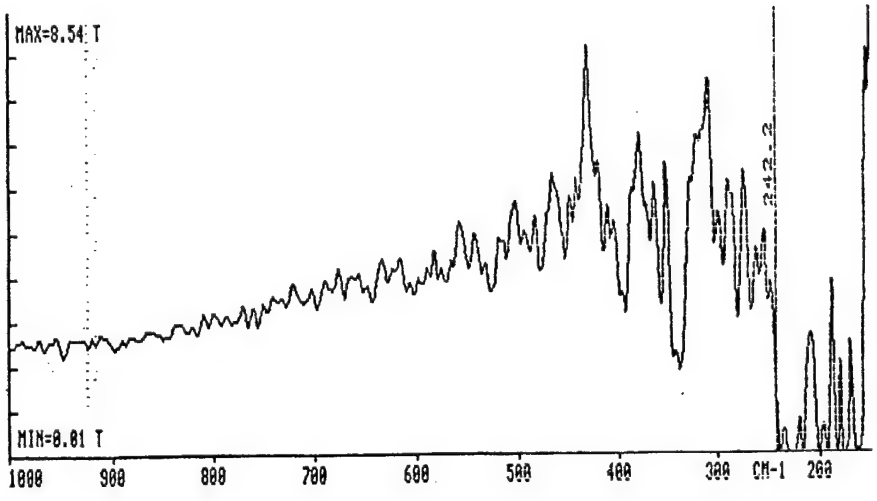

Figure 10. Transmittance vs wavenumbers for IR filter.

II. Integrated Optical Device and Circuit Modeling

BeamPROP: A Photonic Device and Circuit Modeling Package

In this section we discuss our efforts to develop a general software package for design and simulation of photonic integrated circuits (PICs). We continue to develop this software and have at the same time commercialized it.

In the first year of this contract, we reported the initial development of the software and its application to several device problems. These included design of an optical delay line in GaAs and analysis of multimode star coupler devices in polymers. In the second year, we produced a second generation of the software package which included a graphical CAD interface, and advancements in the simulation techniques allowing wide-angle propagation using Padé approximations. Furthermore, we completed our studies of both the star coupler and optical delay line and were able to obtain comparisons with experiments in both cases which corroborated the simulations. In addition, we used the CAD program to assist a redesign of our channel dropping filter, a project which is discussed elsewhere in this report.

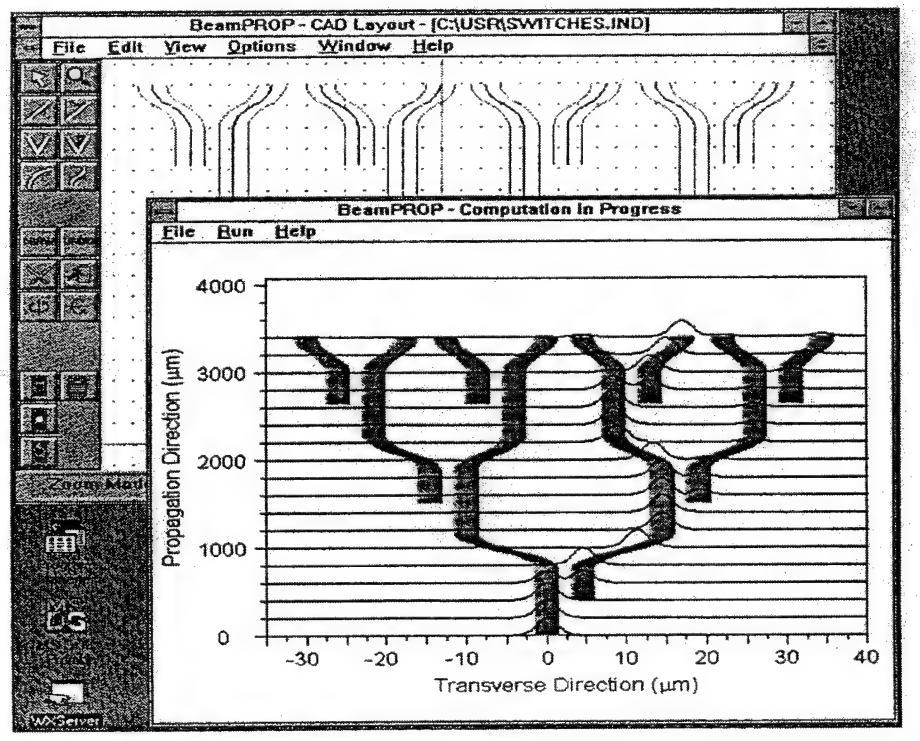

Fig. 11: A screen-view illustration of the *BeamPROP* software running under windows.

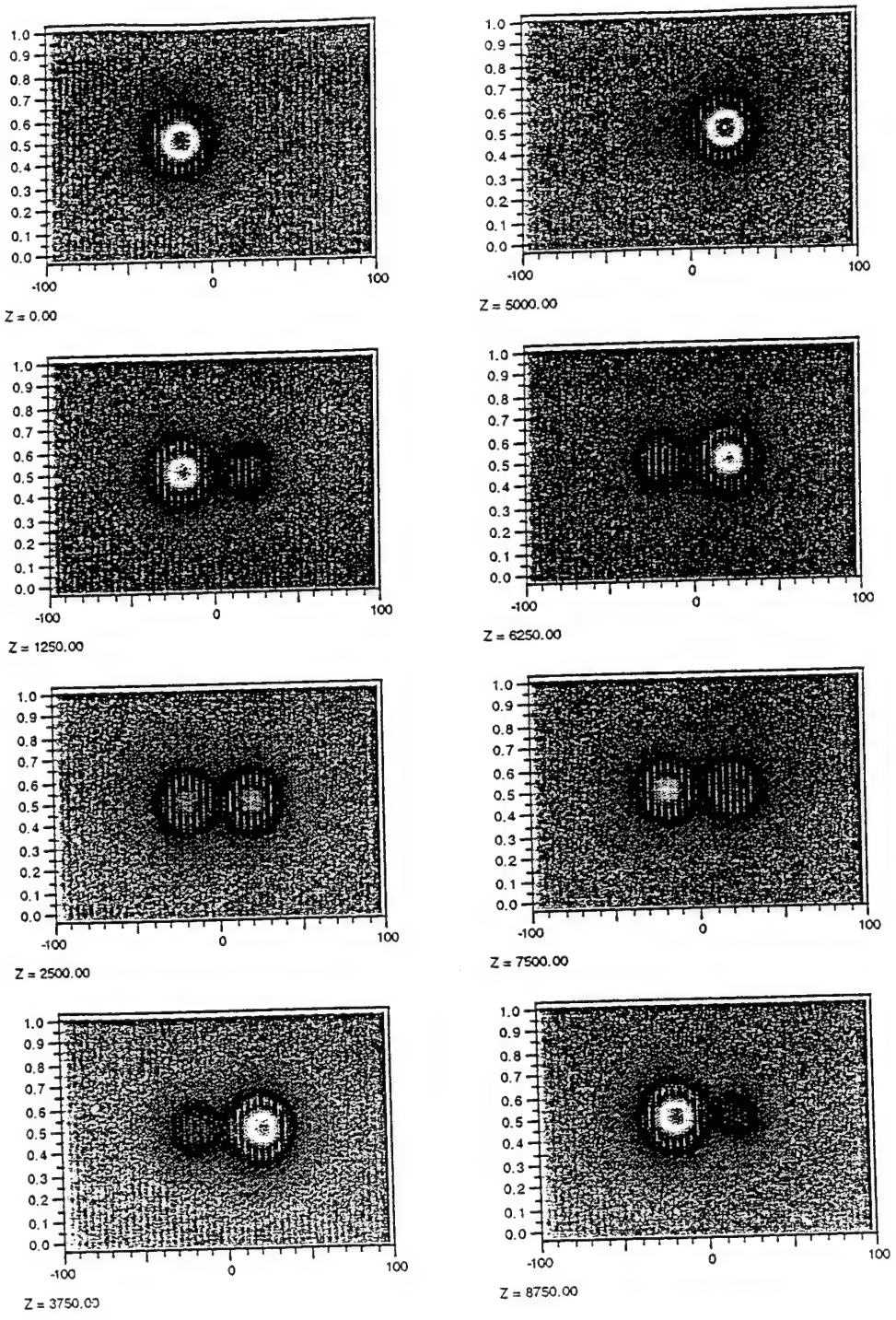

Fig. 12: Three-dimensional *BeamPROP* simulation of two optical fiber couplers.

In the final year of the contract, there have been several additional important developments. First, software development on both the simulation and graphical interface was completed. Columbia was able to transfer the program to a scientific-software house, where it has been developed into a commercial product. Figure 11 illustrates the software running under Windows; several other platforms are also supported. Second, as part of the above development, several new simulation capabilities were added to the software, including support for diffused waveguides, automatic effective index calculations, and full 3-D simulations. The latter task involved exploration of new techniques for efficient and stable 3-D computations. Figure 12 illustrates a 3-D simulation of two coupled optical fibers.

i) Improvements in Algorithms

An important development in the simulation area involved research into the fundamental limits of the beam propagation method with regard to wide-angle propagation. The ability to model or design for wide angles along the propagation direction is a crucial capability for a truly general-purpose modelling program and is a crucial requirement for designing most realistic photonic integrated circuits. In this connection, while the finite-difference beam propagation method using the paraxial approximation has been applied successfully to photonics integrated circuits with shallow angles, it has difficulty in computing practical circuits containing angles $> 10°$. Recent extensions to these techniques based on Padé approximants of the square-root operator in the one way wave equation have made wide-angle propagation possible with a significant improvement in accuracy. However, in order to apply effectively these new techniques to real-world problems, it is necessary to have a thorough understanding of their fundamental limits and how to achieve them.

Much of the previous work in this area has focused on implementation and comparison of algorithms using one or two benchmark examples, rather than considering detailed parametric studies. We have theoretically examined the Padé-based beam-propagation scheme and derived general expressions for angular and truncation error as a function of various waveguiding and numeric parameters. Later, these results were compared with numerical experiments helping us determine scaling rules.

We performed our analytical study by deriving the angular error for the exact solution of the uniform, slab-waveguide problem. In this case, the fundamental mode is inserted into the one-way wave equation obtained from the Helmholz equation using Padé approximants. The result of this derivation is the following formula for the error of a Padé (m,n) approximation:

$$E = q(q/2)^{m+n}$$

where

$$q = [(k - \beta\cos\phi) + i\gamma\sin\phi] / k$$

Our test example for Padé-based numerical experiments was a uniform, slab waveguide tilted at an angle from the propagation direction. This choice is made since the exact solution is known and can be compared with numerical results. Simple measurement of power loss represents the error. Figure 13a presents this error as a function of grid-size, with refractive index difference as a parameter. The error approaches a constant error limit, which is plotted for different angles in Fig. 13b and fitted with $\sin^4 \phi$, (following the derived expression).

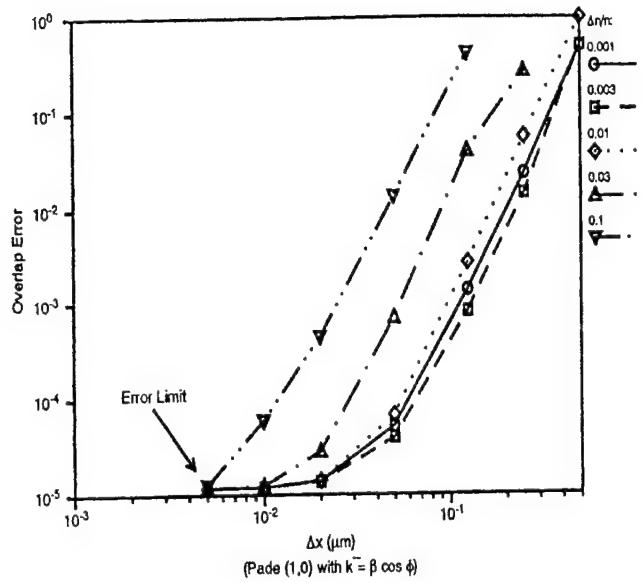

Fig. 13a

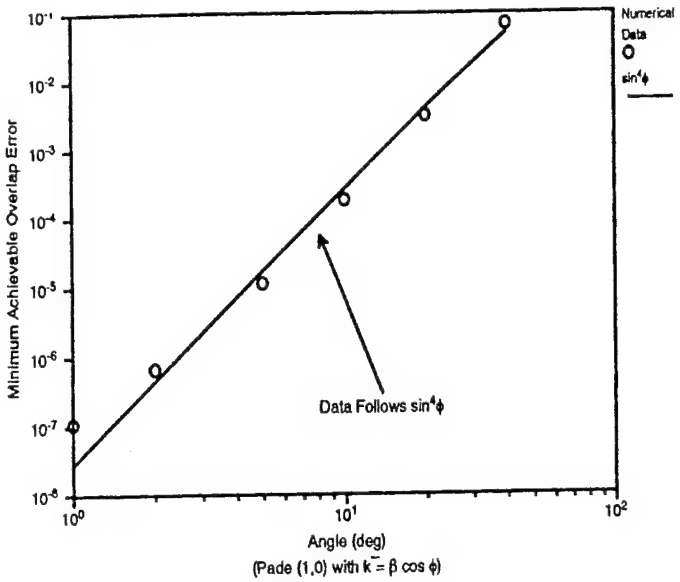

Fig. 13b

ii) Graphical User *BeamPROP* Program

In addition to technical improvements, we have added a unique graphical interface to the package which integrates CAD layout of waveguide circuits with the simulation. The CAD system has been designed specifically for photonic circuits, and incorporates special features which allow great flexibility in exploring design modifications and their effects on performance. This technology has been shared with collaborators at AlliedSignal, Inc., and has interested researchers at IBM as well.

iii) Use in Actual Device Simulation

Our simulation capability has continued to be an important part of our overall program. As discussed elsewhere, we used *BeamPROP* extensively in our redesign of the channel dropping filter.

In addition, in our efforts to improve our fabrication process to produce large PIC devices such as a transversal filter, we have used *BeamPROP* to explore the sensitivity of the Mach-Zehnder interferometer and other devices for fabrication errors.

In particular, working with Allied we have explored the design of highly multimode star couplers for fabrication in polymer materials. In collaboration with H. Fetterman at UCLA, we have designed an optical delay line (see Fig. 14). Finally, we are currently using the program to assist our work on wavelength demultiplexers by considering the design of low divergence adiabatic tapers. The following is a brief description of our work in using *BeamPROP* for designing multimode star couplers.

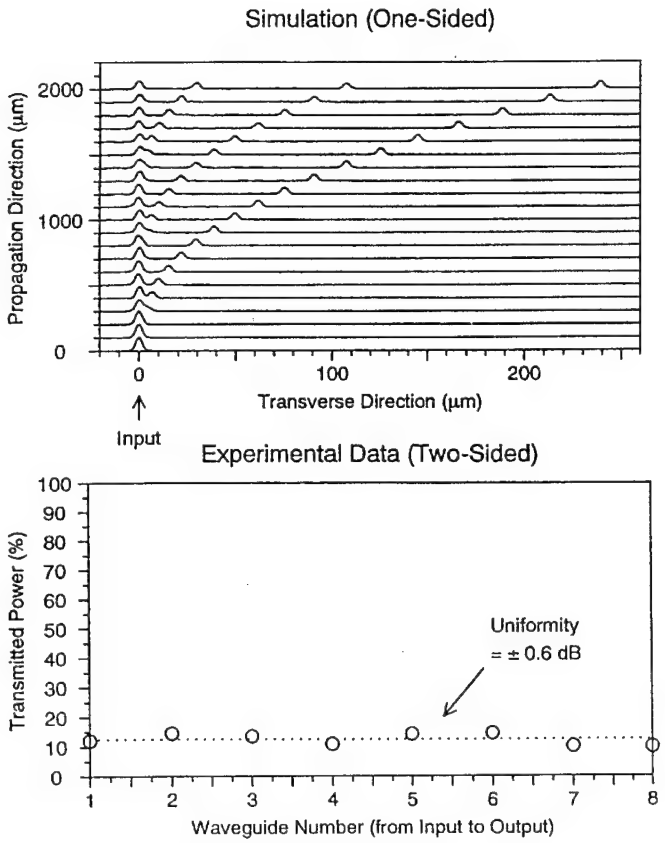

Fig. 14. Optical delay line simulation and experimental data.

Our application of *BeamPROP* in the understanding of light propagation in highly multimode star couplers was done in collaboration with AlliedSignal, Inc. and was cosponsored via partial student support by AlliedSignal, Inc. and the NCIPT program. The fundamental work has been completed during this period, and has resulted in a good understanding of factors that influence output uniformity and device length requirements. Furthermore, we have developed a set of empirical rules that describe these effects and allow simplified device design. This work has been published in the Journal of Lightwave Technology.

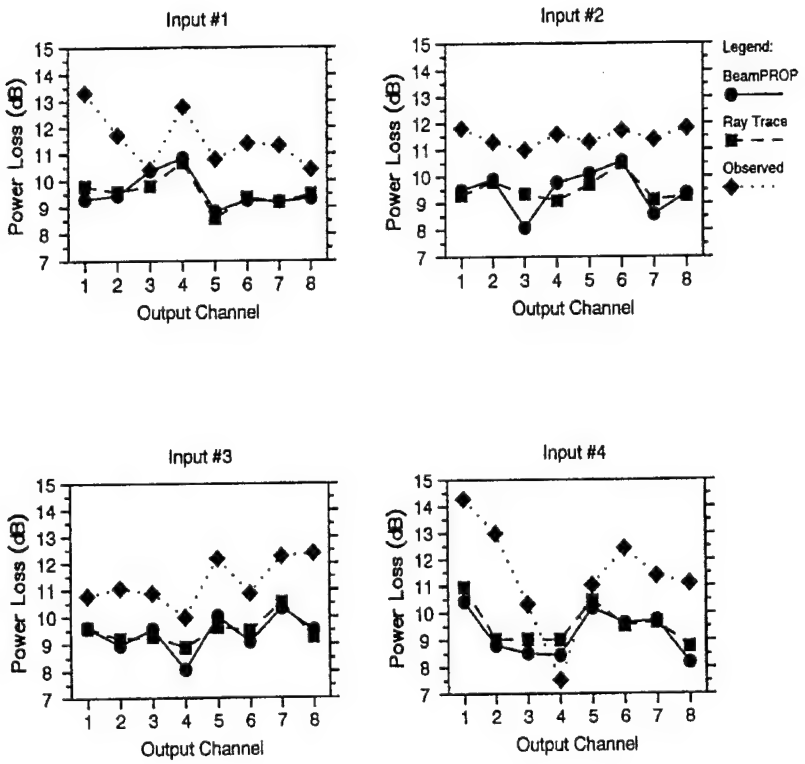

Fig. 15. 8x8 Star Coupler output uniformity.

In addition to this basic study, we have collaborated with AlliedSignal, Inc. to model a large, 8 x 8 star coupler of a specific design which they subsequently fabricated and tested. The results of this study are shown in Fig. 15 along with the experimental observations, as well as additional

calculations performed using a ray-tracing approach by AlliedSignal, Inc. The graphs show the relative power in each of the eight output ports, when excited by each of the left four input ports (by symmetry the right input ports are identical). We note excellent agreement between our technique and the ray-tracing model. Furthermore, the theory exhibits the general trends portrayed by the experiment, although there are a few significant discrepancies, particularly for input #4. We are presently investigating the origin of this effect, but it seems to be tied to some aspect of the experiment that was not foreseen and included in the theory, since the two independent models yield similar results.

III. Writing Technology

A. Laser Wet Etching Writing

We have succeeded in using our laser wet etching system for the rapid prototyping of various passive and active devices in GaAs, namely, linear waveguides, bends, Y-branches, tappers, couplers, delay lines, polarization modulators and Mach-Zehnder interferometric modulators. These results have been published in the Journal of Lightwave Technology. Our next goal is to integrate these elements to fabricate large-area, interferometry-based devices for optical signal processing, such as transversal filters (see Fig. 16) and wavelength multiplexers. For this purpose, we need to reproduce a large amount of the same elements on one complex device. Hence, our recent work is concentrated on improving the reproducibility of our laser etching-writing technique.

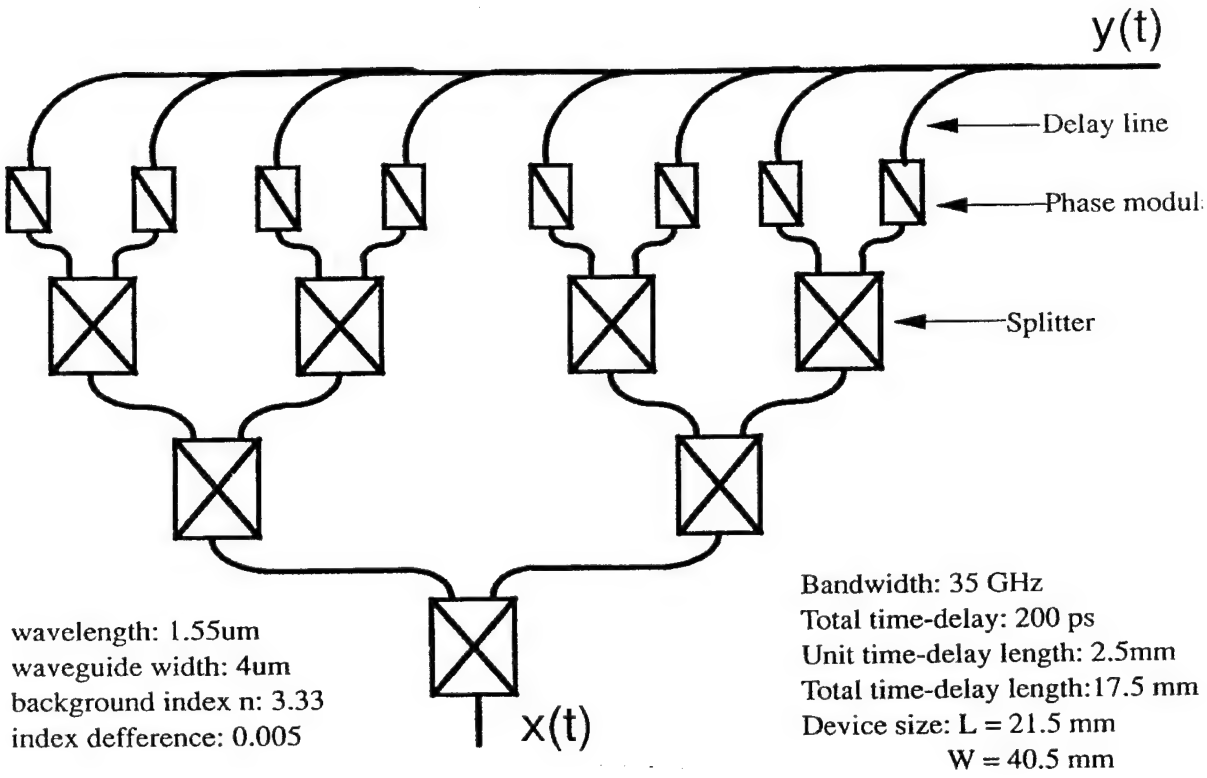

Fig. 16: Schematic and specifications for our optical transversal filter.

We have determined and enhanced the reproducibility by improving and formalizing our fabrication and measurement techniques. In fabrication, we discovered that by processing the sample in the etching solution for a sufficiently long time we can obtain good symmetry and uniformity of the waveguides. We found that simple transmission measurements of optical output power were not accurate due to the Fabry-Perot resonances between the two facets of the sample. To eliminate this effect, we used an approach based on wavelength-sweeping, which also avoids the problem of index change due to temperature fluctuation. We found that the output power of the linear waveguide has a variation which is less than 5% and a Y-branch variation less than 10%, including a 3% measurement error (see Fig. 17). Also, we fabricated a polarization modulator with a 100% success rate. We are currently working on obtaining better reproducibility of the Mach-Zehnder interferometric modulator.

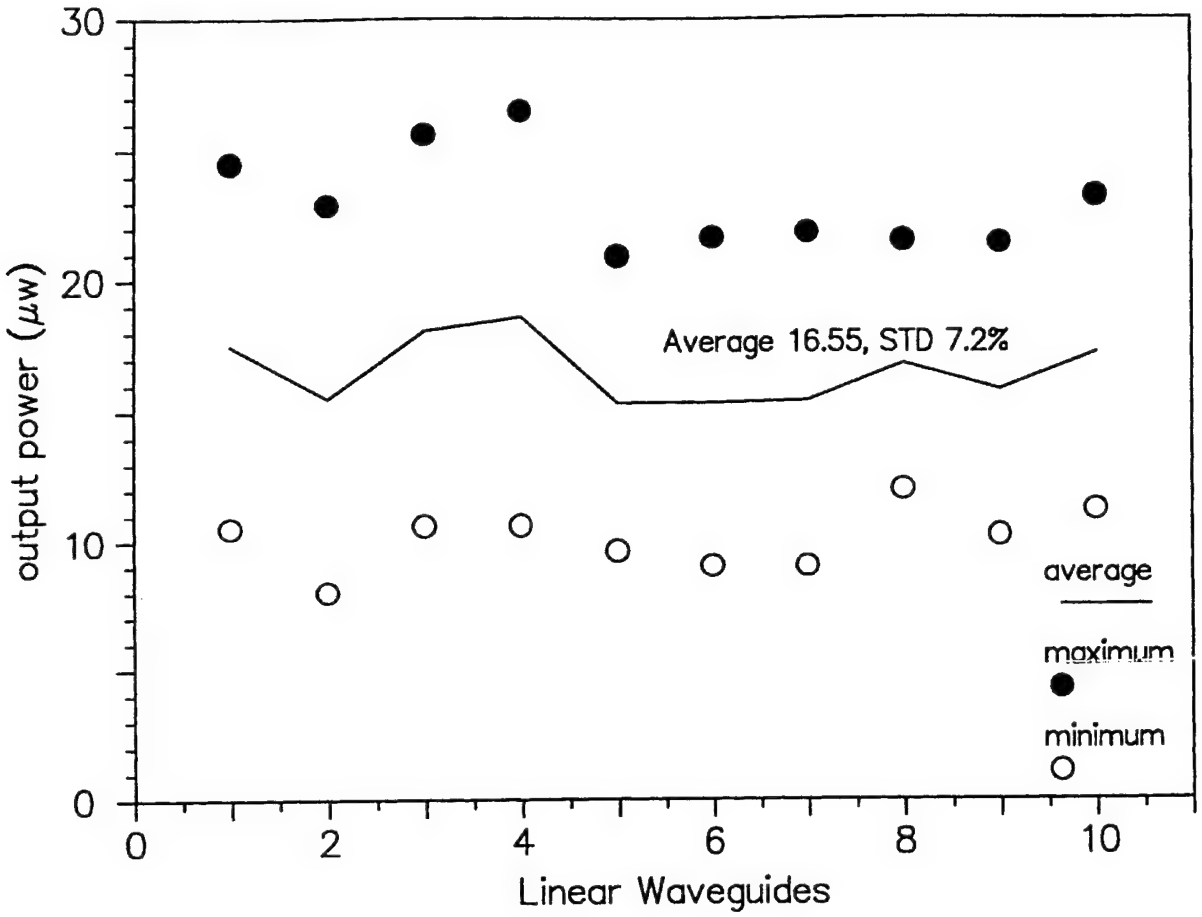

Fig. 17: Reproducibility study of linear waveguides. The maximum and minimum correspond to peaks and valleys of Fabry-Perot oscillations, and the standard deviation (STD) for each waveguide is 3.7%.

B. Wet Etching of Facet Grating

We have developed a capability for wet etching of gratings on end facets of (100) GaAs, cleaved along the (011) set of planes. These are samples with GaAs, $Al_{0.1}Ga_{0.9}As$ epilayers grown on them for waveguide structures. The importance of end facet grating fabrication stems from its applicability to device fabrication, such as for demultiplexers.

The epilayers are doped to $10^{16}cm^{-3}$ material. The gratings are fabricated via holographic interference with UV light, using HNO_3:HCl:H_2O::1:4:50 as etchant, which has been shown by our group to provide the best feature resolution for our laser-writing waveguide fabrication.

Figure 18 shows an SEM photograph of a grating on a GaAs end facet. Notice the good quality of the grating on the GaAs epilayer.

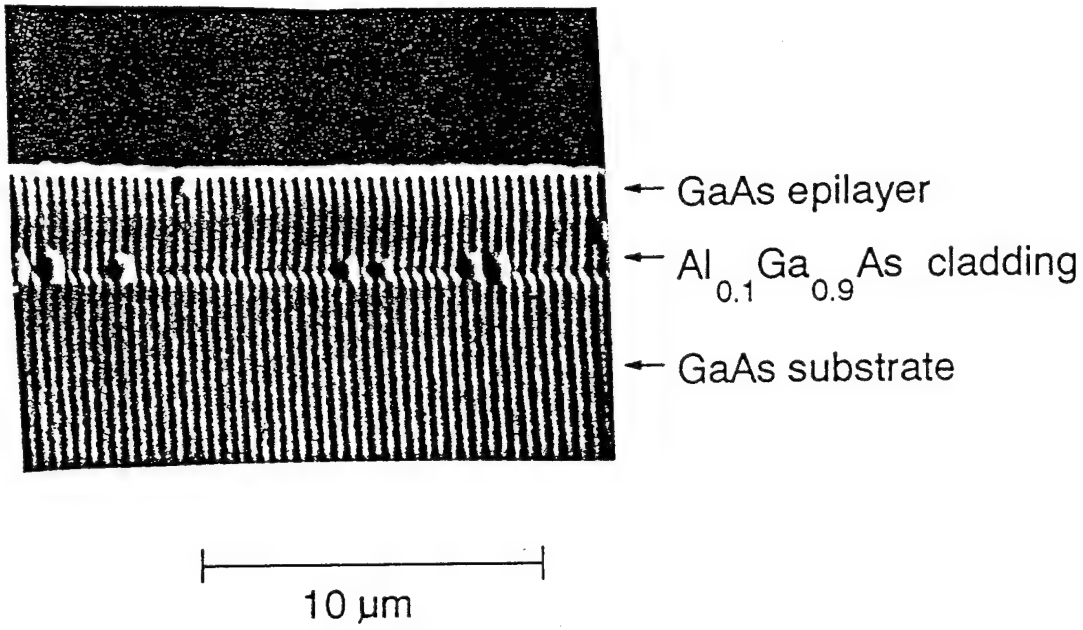

Fig. 18. Grating on facet fabricated by wet etching.

C. Writing with Photoresist

Laser-direct writing techniques have been developed in this lab for several years. This knowledge is now being applied to direct-exposure techniques of photoresist with the hope of providing a new flexibility in the making of both positive and negative masks using conventional lift-off processes. In addition, and perhaps more importantly, with the use of a negative resist, this technique allows for the rapid direct patterning onto a semiconductor, as well as a great variety of other materials.

Recent progress on this project has included software development which has increased our ability to draw complex patterns (e.g. including bends and circles) of higher quality (see Figs. 19a and 19b).

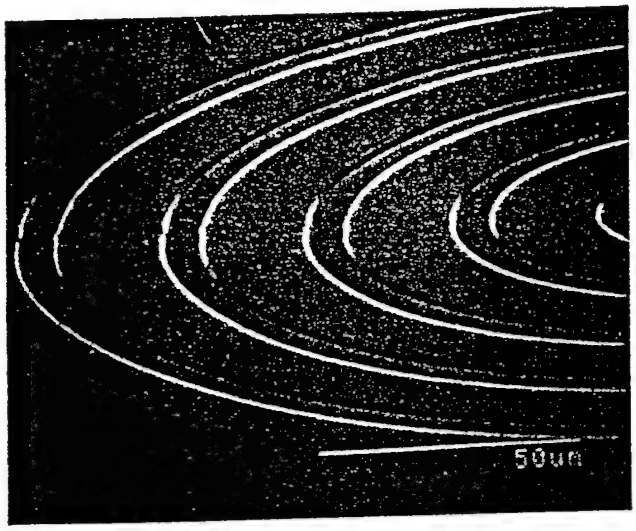

Fig. 19a

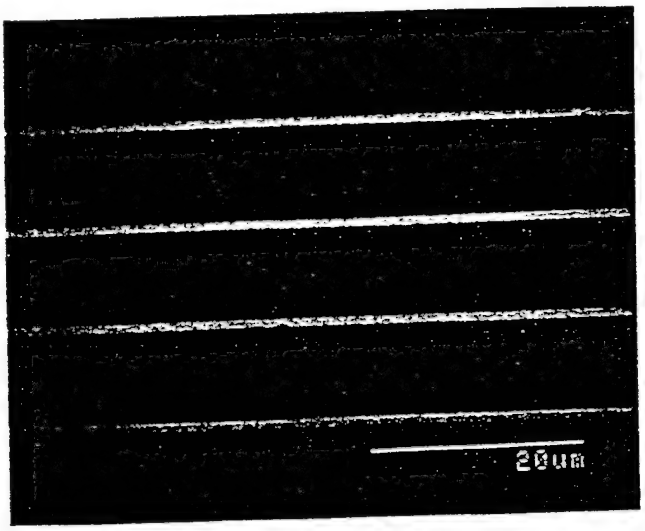

Fig. 19b

In addition, we have recently begun to explore etching techniques to be used with such PR patterned features on our way to developing our device-creation process. Using a wet-etch process we have obtained patterns with critical dimensions on the order of 3 μm, which is more than suitable to assure single-mode optical performance (see Figs. 20a and 20b).

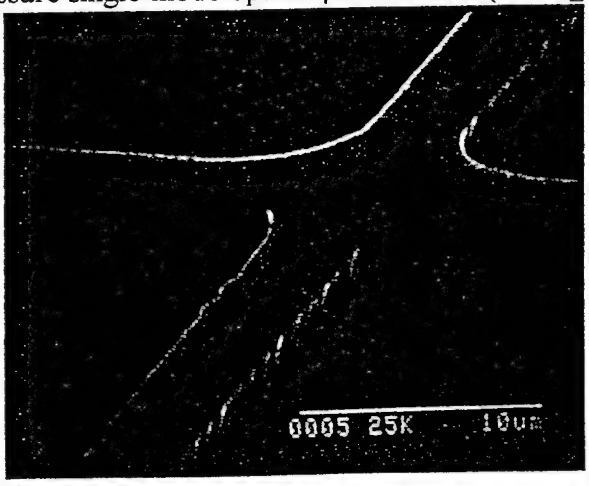

Fig. 20a

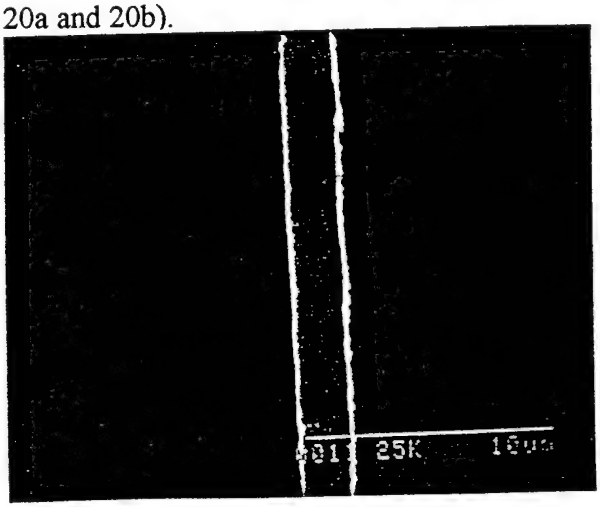

Fig. 20b

D. Fabrication of an InGaAs SQW Circular Ring Laser by Direct Laser Patterning

Circular ring lasers are of considerable interest for monolithic optoelectronic-integrated-circuit (OEIC) applications. Since these lasers do not require the use of a cleaved facet for output coupling, they can be conveniently integrated for OEIC applications, and on-chip laser output coupling can be achieved via the use of an evanescent coupler, Y-branch splitter, etc. The etching technology used for the pattern transfer of the ridge-waveguide structure of these lasers is crucial to their operation, since the definition and uniformity of the etched sidewalls depend on the characteristics of the anisotropic etching. The crystallographic etch-rate variation in conventional wet etching makes wet etching undesirable for the etching of a circular ridge-waveguide structure, the side walls of which utilize a continuous variety of crystallographic orientations. In addition to the etching step, the use of a simple, rapid fabrication procedure can facilitate the prototyping and testing of these devices.

We have demonstrated that high-performance ring lasers can be made using novel laser direct-write lithography for the pattern definition. This laser-based lithography provides a flexible and easy way of modifying the optical structures while the optimal design of the devices is being established. The ring lasers were fabricated using an MBE-grown 80Å-strained-layer $In_{0.25}Ga_{0.75}As$ quantum-well heterostructure material. The ridge-waveguide for the circular ring is 200 μm in radius, 15 μm in width, and has a 1000-μm long Y-branch output coupler. A two-layer photoresist process was developed which utilized two commercially available photoresists with different absorption wavelengths to achieve the desired undercut structure, which is necessary for metal liftoff. The pattern in the top photoresist layer is defined by a focused UV beam scanned across the substrate with a computer-controlled, high resolution X-Y stage. Cryoetching, a dry-etching technique, is applied to defining the ridge waveguide structure. This crystallographically independent etching process

yields uniform ring patterns and smooth side walls.

Our fabricated ring laser had a threshold current of 270 mA, corresponding to 794 A/cm^2, and emits ~ 14 mW of single-frequency output. The slope efficiency over the range 300-500 mA was 64 W/A.

IV. Processing for Ultra-Electronic Devices: Cryogenic Etching for Low-Damage, Sub-Micron Processing of MQWs

Under the last contract (AFOSR/ARPA #F9620-89-C-0088), we developed a dry etching process for GaAs and related compounds in which an excimer laser is used to activate a condensed layer of chlorine on the surface of the semiconductor and to remove etching products from the reaction area. The restriction of the reactive species to the surface, as well as the limitation of the product desorption to the illuminated area, yield an anisotropic etching without the need for highly energetic particle beams which damage sensitive MQW materials. In the initial work, the technique was carefully characterized in terms of process parameters. This work has recently published in both Applied Physics Letters and the Journal of Vacuum Science and Technology. In addition, gold masks patterned by liftoff were used to demonstrate micron-scale patterning, and silicon nitride and silicon oxide were tested for suitability as mask materials.

We have continued our work on this important technology by first demonstrating sub-micron pattern-transfer with this technology using e-beam patterned silicon-nitride masks. In addition, we have applied the technique to the fabrication of a quantum-well stripe laser. We have also performed detailed measurements using photoluminescence on MQW structures and on Schottky devices fabricated on GaAs etched by our technique to demonstrate low damage. Finally, we have made

several fundamental improvements to our apparatus and process. The above work is described in the following.

A. Pattern Transfer

One of the ultimate goals of this project is to etch feature of submicrometer dimensions. The first step towards this goal is to find a suitable surface mask. The gold surface masks we have been working with up to now are unsuitable for high resolution applications because they often erode on the sides and because of the resolution limits of conventional lift-off lithography. The requirements for effective masking materials are resistance to the chlorine environment and excimer laser irradiation and the ability to be patterned to submicrometer dimensions.

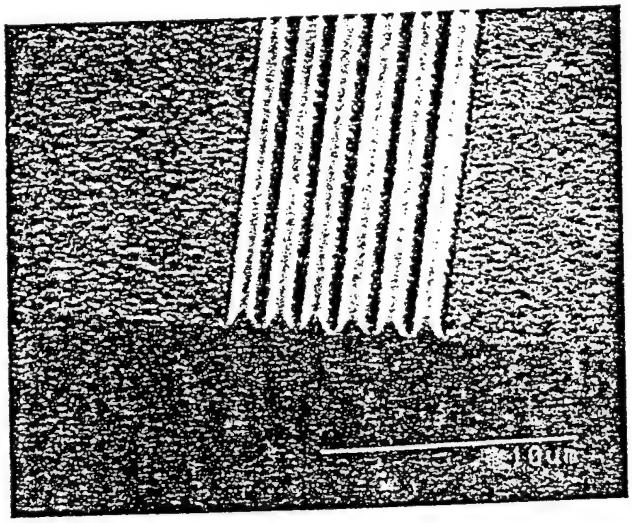

Figure 21. SEM of sub-micron features etched in GaAs using the low-damage cryogenic .

For our studies of submicrometer etching, we used a Si_3N_4 mask patterned by electron beam lithography and reactive ion etching by Cornell University's National Nanofabrication Facility. The detailed results, along with some micrographs, are discussed in our Journal of Vacuum Science and Technology article. Figure 21 shows the cross section of a feature etched on the GaAs (110) surface.

We are able to etch features a half micrometer wide with aspect ratios of greater than one. A major finding is that the sidewall slope is independent of both the surface being etched and the orientation of the feature on the surface.

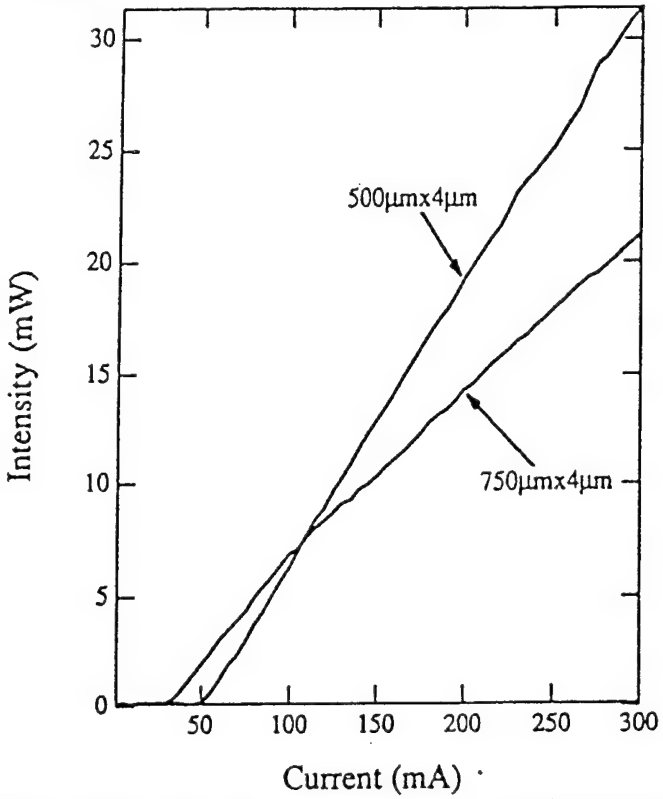

Figure 22. LI characteristic of a quantum well ridge laser etched using the low-damage cryogenic etching technique.

To test the suitability of this etching for device fabrication, we collaborated with Prof. Wen Wang's group at Columbia to apply our etching process to etch a mesa for a single quantum-well ridge waveguide semiconductor laser. Figure 22 shows the LI (light out-current in) characteristics of the laser. The performance of these lasers is comparable to that of lasers fabricated by wet etching. Since wet etching of II - V semiconductors is heavily dependent on crystallography and doping type and level, our low temperature etching process is more reliable for achieving micrometer scale structures. To complete this project, several technical challenges needed to be overcome. Most significant is the requirement for a uniform etch depth, which required that the excimer laser beam

have a uniform intensity profile. This was accomplished through careful re-design of our optical beam delivery system.

A new etching chamber and load lock system, sketched in Fig. 23, has been installed and tested during this contract. The purpose of this apparatus is to accomplish sample transfer without exposing the etching chamber to the atmosphere. The new etching chamber is pumped by a turbo pump and during etching, the background pressure is about 10^{-7} Torr. The installation of the load lock system allows us to repeatedly do experiments without breaking the vacuum; as a result, we can obtain better surface morphology. We point out that a load-lock system is important for low temperature etching processes, as many contaminants, such as moisture and residual etching products, tend to absorb on the sample surface at low temperatures.

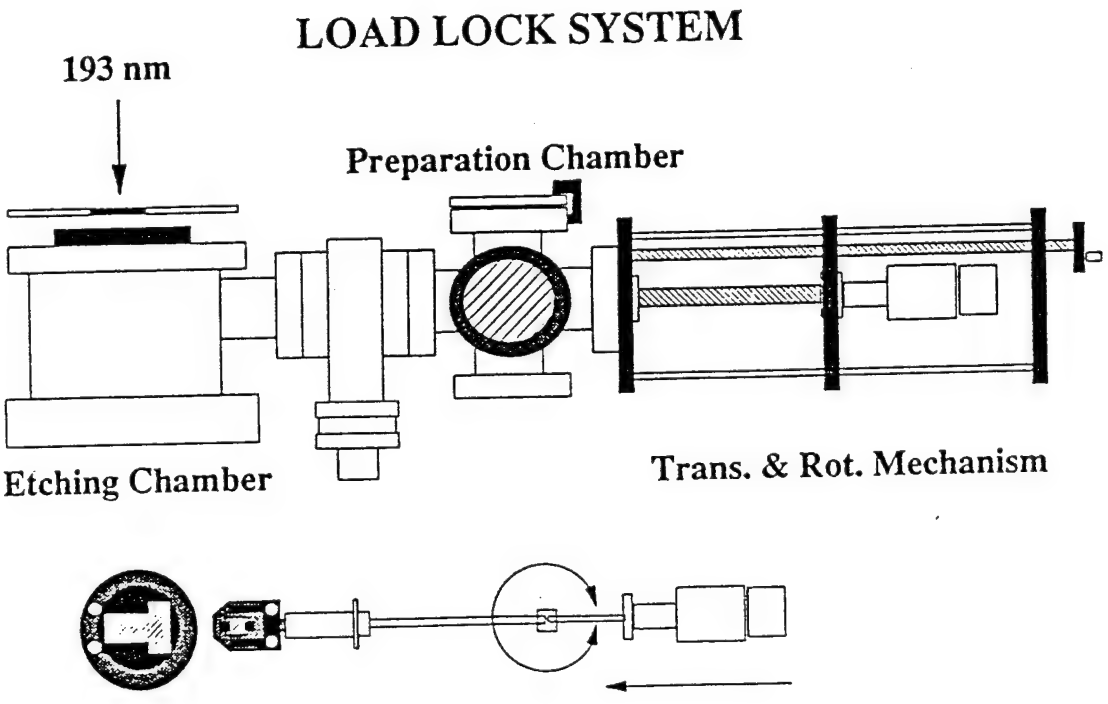

Figure 23. New vacuum chamber and load lock for cryogenic etching system.

We explored the effects of the addition of rare gases to the etching chamber, as described in the last report. For the addition of Xe, Kr, and Ar, we saw an enhancement of the etch rate to about twice the normal etch rate with increasing rare gas partial pressure, and then a quenching of the etch rate with further addition of the rare gas. The addition of He or Ne causes no enhancement of the etch rate. Instead, they immediately cause a decrease in the etch rate. We suggest that the etch rate enhancement is attributable to a parallel channel for generating Cl atoms through the formation and decay of excited rare gas halide molecules. We have also found that the addition of rare gases results in a noticeable improvement of surface morphology.

B. Sub-Micron Patterning and Etching

Unfortunately, submicrometer lateral resolution by using a Si_3N_4 mask leads to an undercut, which we attribute to strain-induced chemistry, thus severely limiting the lateral resolution obtainable using this mask, making it impossible for us to transfer patterns of less than 0.5 μm linewidth into the sample. To eliminate this problem, we used a mask consisting of 500 Å Au on top of a thin (~50 - 200 Å) layer of Cr or Ti to promote adhesion of the Au. This masking also has several advantages over the Si_3N_4 mask: it is deposited practically stress free and is capable of being patterned by lift-off lithography, which does not require a dry etch process (which may cause surface damage).

Figure 24 shows the etching of 0.2 μm features patterned by the Au/Cr mask. This photograph clearly shows that our etched feature profiles have no crystallographic dependence. In Fig. 25, we show an array of 0.5 μm boxes that were patterned with a Au/Ti mask fabricated using ion beam lithography and etched for preliminary investigation of the suitability of our etching for the fabrication of quantum boxes. This structure is similar to that of a proposed quantum box laser,

which is predicted to have a lower threshold current than conventional semiconductor lasers.

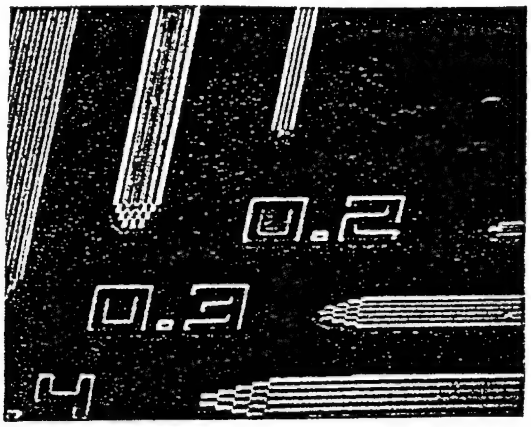

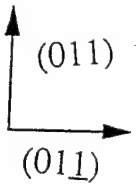

Equal Resolution Along (011) and (01$\underline{1}$) Directions.

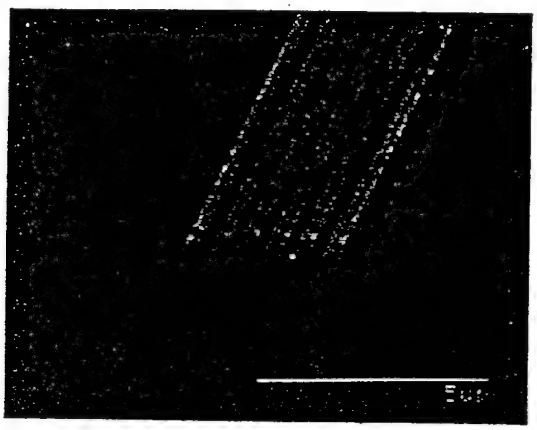

0.3 μm Line/Space Pairs

Fig. 24. High-resolution etch using Au/Cr mask.

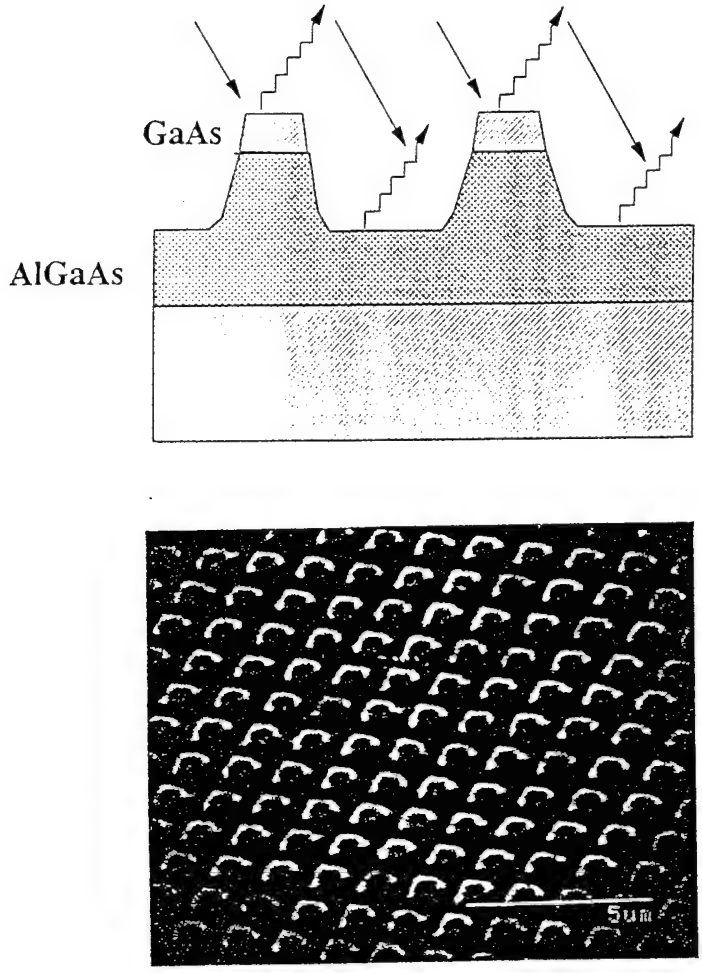

Fig. 25. Characterization of the photoluminescence of cryoetched submicron dots.

C. Determination that Cryoetching is Indeed Damage Free

An important advantage of the new technique of laser cryoetching is that it is both directionally anisotropic and yet purely chemical in origin. That is, since it does not rely on bombardment by massive particles to achieve etching, material damage should not result in damage

of the etched material. Moreover, the high flux of atomic species or carriers that is generated by laser irradiation makes it possible to obtain high surface-reaction rates. Etching resolution in such a neutral-atom, laser-assisted method is determined both by the quality of the imaging optics and by the confinement of the reactive species to the illuminated surface area.

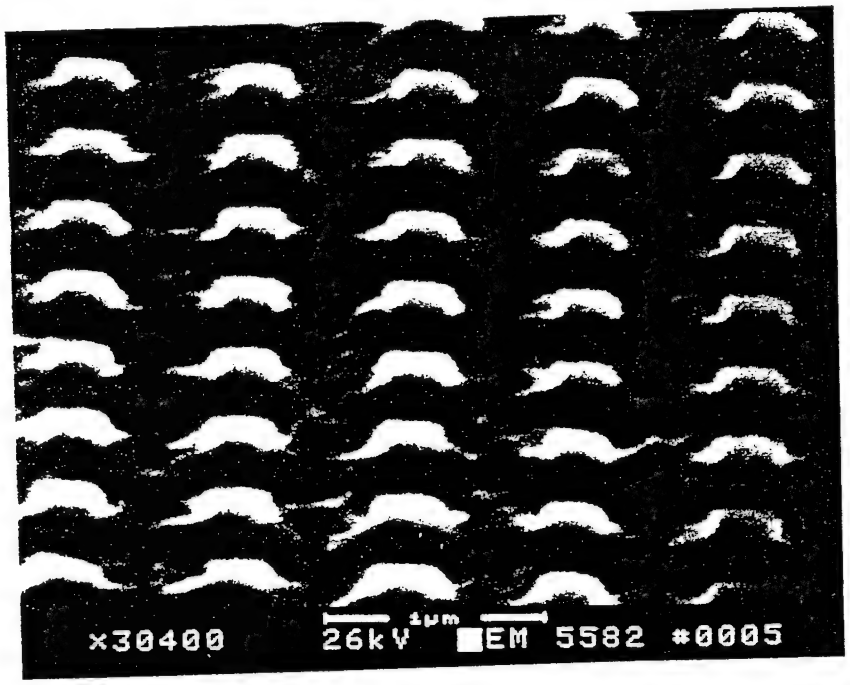

Fig. 26: An array of etched 200-nm quantum boxes. The Ni etch mask is still on the sample.

In order to quantify any process damage produced in cryoetching, we chose to use photoluminescence since it samples the radiative efficiency of the patterned submicron structures. In our case, a test substrate was designed and grown commercially for use with photoluminescence probing. Specifically, a test pattern, consisting of arrays of squares fabricated on a multiple-quantum-well substrate, was etched into the semiconductor surface. The substrate consisted of three 50 Å GaAs quantum wells, separated by 250 Å $Al_{0.3}Ga_{0.7}As$ barriers, with a 50 Å GaAs layer cap. All epitaxial layers were undoped, grown on a SI GaAs(100) wafer by MOCVD. Etching through the

multiple quantum wells typically required 15 minutes. The test pattern consisted of 200 μm square arrays of smaller squares with dimensions ranging from 250 to 2000 nm (full width), with a pitch of three times the size. The surface mask was fabricated using electron-beam lithography to pattern a 200 Å Au/ 50 Å Cr thin film. Similar masks of 700 Å Ni were also fabricated. Figure 26 presents an electron micrograph of an array of 200-nm quantum boxes, etched to a depth of 0.12 μm, showing that the mask pattern has been faithfully transferred into the sample.

One accepted procedure for measuring the process damage in etched samples is to compare their luminescence efficiency to the luminescence efficiency of an accepted standard fabricated by an etching technique which is commonly accepted to be damage-free, typically wet etching. In our case, quantum boxes were also fabricated by wet etching in a (1:8:50) solution of H_2SO_4:H_2O_2:H_2O. In this wet etching (as is generally seen), crystallographic anisotropy of the wet etching results in significant undercutting. Specifically, the etched feature is rectangular, despite the square etch mask, indicating that the wet-etch rate is different in the two crystallographic axes. While this effect precludes more general use of wet etching, with care we were able to obtain suitable damage-free samples down to ~ 300 nm in dimension.

In general, the quantum-well luminescence peak energy of the etch-defined quantum structures exhibited a blue-shift as the feature size decreased. For example, for 500 nm features, this shift was about 10 Å (~ 2 meV). As the feature size decreased, the luminescence spectra remained symmetric and the peak width remained constant (7.0 - 8.0 meV, FWHM), indicating that variations in the feature size and sidewall quality are negligible.

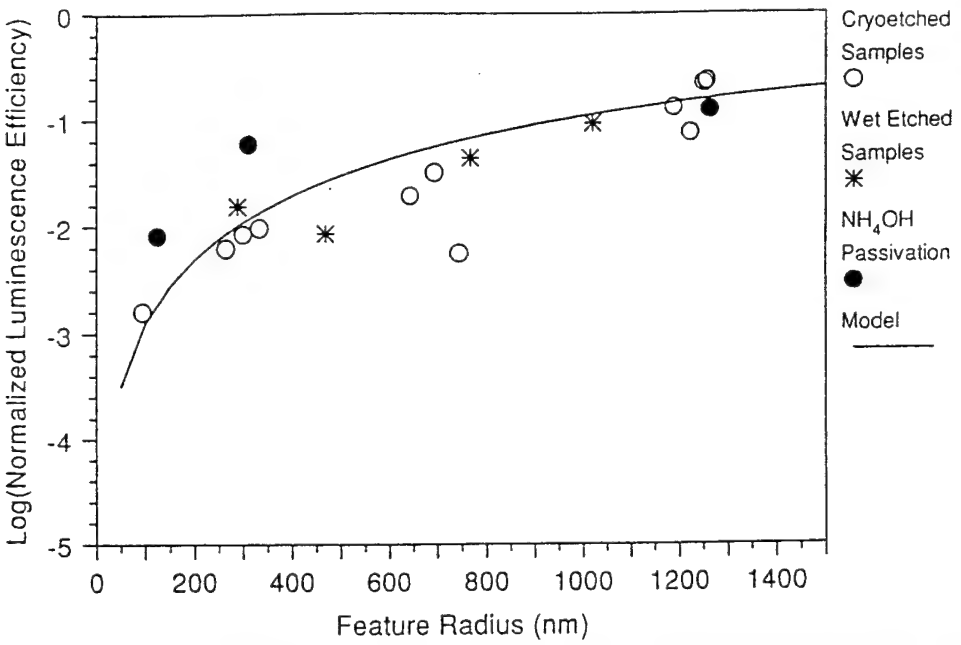

Fig. 27: Normalized luminescence efficiency as a function of feature radius for quantum boxes fabricated using cryoetching and wet etching. The solid circles represent samples passivated by using NH_4S.

Figure 27 shows the normalized etched feature luminescence signal as a function of etched feature size for the wet-etched standard and for cryoetched samples. For the model curve shown in this figure, the feature size is defined as the radius of the circle having the same area as the etched feature. This figure also includes PL from the comparison samples obtained by wet etching. The cryoetched feature data represent the results of four experiments, indicating that the results are consistent.

Both the laser- and wet-etch data have the same luminescence efficiency, indicating that our etching induces little or no damage to the feature sidewall. Note that even though the wet-etched and cryoetched sample have the same luminescence efficiency, the luminescence signal from the cryoetched sample is much greater than the luminescence signal from the wet-etched sample. This occurs because the wet-etched sample has a smaller fill factor due to process undercutting. The lack

of damage is a direct consequence of the purely photochemical nature of this etching. Because of this lack of *damage*, there is not any "cut-off" radius below which no luminescence is detected, as is commonly seen in ion-etched samples.

D. Damage Study in Magnetron-Induced Etching Systems

Recently our work in techniques to probe processing damage attracted the attention and collaboration of a group at Fort Monmouth, who have worked extensively in the area of magnetron-induced etching (MIE). At their suggestion, we began a joint project to investigate adjusting plasma conditions to reduce ion damage during this important form of commercial etching.

In the experiment, the same protocol and experimental techniques were used to assess process damage as used in laser cryoetching. For example, Fig. 28 shows the logarithm of the measured quantum-box luminescence efficiency as a function of the feature effective radius for 200 W/30 V biased samples, etched to different depths. The effective radius is defined as the radius of a circle that has the same area as the average area of the quantum boxes in each constant-feature-size array. For the larger feature radii, the luminescence efficiency of all the samples is about the same. However, for the smaller feature sizes, the quantum-box luminescence efficiency decreases as the exposure time increases. These results indicate that, in general, MIE can induce damage to the quantum box sidewall, and that this damage increases as the sidewall is exposed to the plasma. The solid line in this figure represents an application of the previously described model, based on drift-diffusion of minority charge carriers, of the luminescence efficiency in an array of quantum dots.

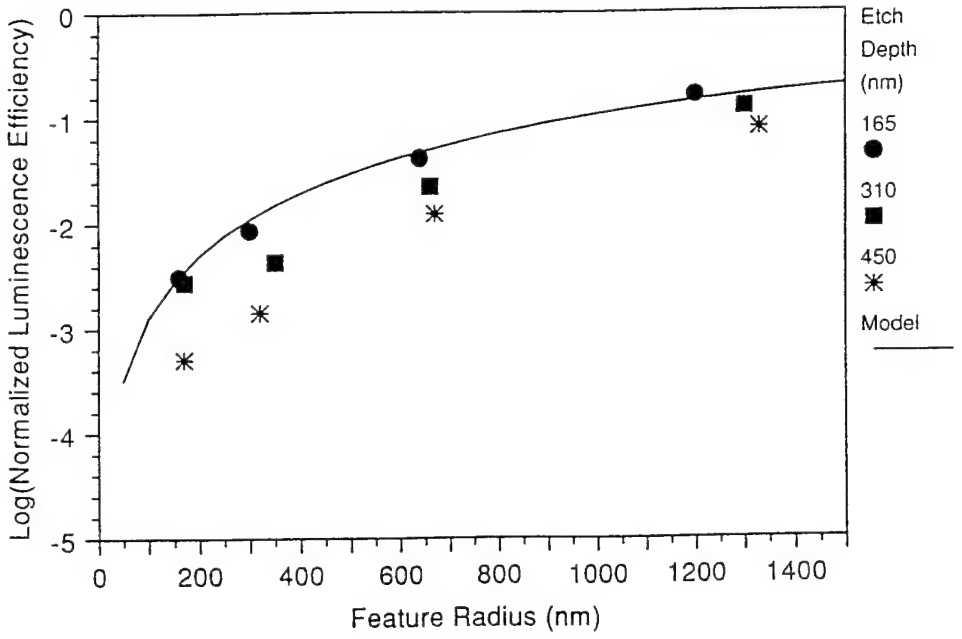

Fig. 28: Quantum box luminescence efficiency for quantum boxes etched to different depths using 200 W (30 V bias) MIE.

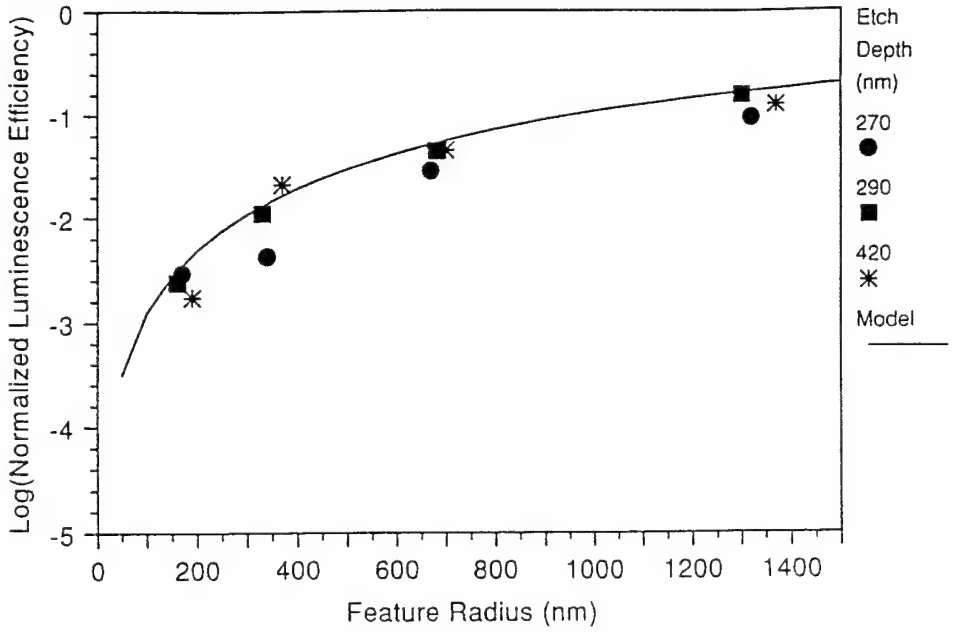

Fig. 29: Quantum box luminescence efficiency for quantum boxes etched to different depths using 400 W (75 V bias) MIE.

However, we have recently found using our PL probe that by paying sufficient attention to the plasma conditions, damage can be eliminated or at least be significantly reduced. Compare Fig. 28, for example, with the logarithm of the luminescence efficiency as a function of feature radius for samples etched with a somewhat higher bias, i.e. 75 V (400 W RF power), which is shown in Fig. 29. In this case, the luminescence efficiency is essentially independent of the etch depth and is very close to the modelled curve and the wet-etched sample data. This behavior indicates that etching with the higher bias voltage does not significantly damage the quantum-box sidewalls. *Thus "voltage-tuning" may offer a valid approach to reduce process damage*. Etched sample surface damage measurements have shown that increasing ion-bombardment energy in chemically-assisted etching reactions may leave a less-damaged surface, due to the increased removal rate of the damaged material. That argument is not valid for this particular situation, though, because our measurements are sensitive to damage to the sidewall surface, where the material removal rate is negligible. In our case, the lack of damage may be due to the increased anisotropy of the ions at higher sample bias; increased deflection of the ions into the sidewall due to image potential on the sidewalls on local nonuniformities of the electric field would generate larger damage at low bias. Because of the importance of this result to scaled-down device technology, further experiments are planned.

E. GaSb Etching

In addition, because of the applications of this research to the fabrication of electron devices, we have made an initial study of the etching of the GaSb and InAs materials which are used in advanced resonant-tunnelling devices. Specifically, these measurements have focussed on determining the etch rates of these materials and comparing them to GaAs. In order to measure the

etch rate of these materials we initiated a collaboration with Prof. McGill's group at CalTech who agree to grow the needed samples. As shown in Fig. 30, the former's etch rates are comparable to GaAs and, hence, etching of devices based in these materials appears feasible. Further studies are planned for our follow-on contract.

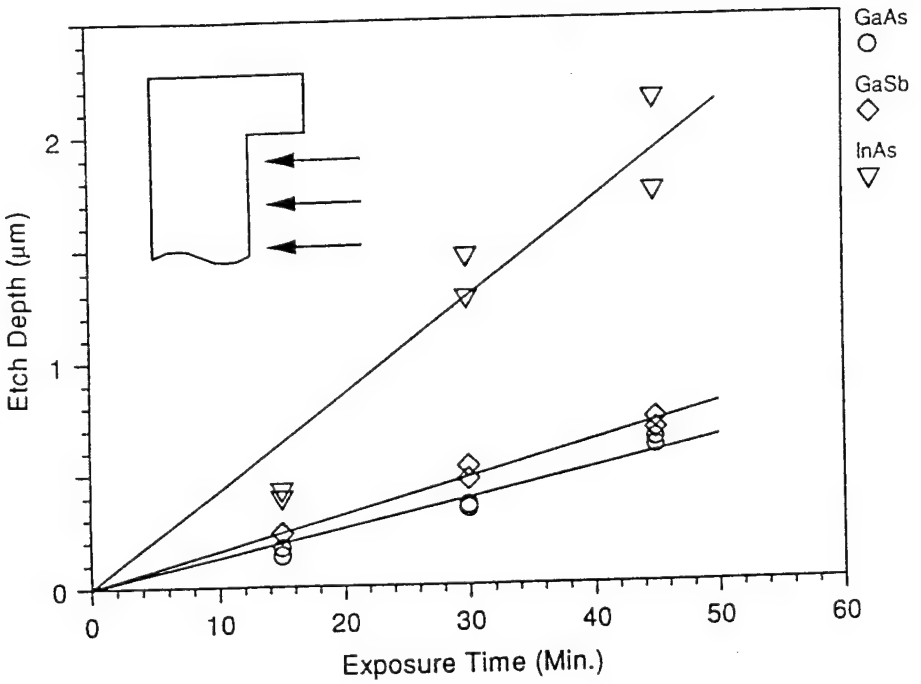

Fig. 30: The measured etch depth versus etching time of GaAs, GaSb, and InAs.

F. InGaAs/GaAs Etching

A second material system that is used in the Ultra Program has been that of MQW of InGaAs in GaAs. We have also investigated the etching of this material. *A priori* we initially expected that the presence of the indium in the material would lead to problems in both the etch uniformity as well as the anisotropy; an effect seen in ion etching, for example. In experiments, both the basic etch rates were characterized and found to be nearly identical to that of pure GaAs, and the etch uniformity was also examined with SEM studies and also found to be satisfactory. In addition, in this case we were

able to test the performance of electronic devices made of this material via the fabrication of laser diodes. These structures were made with both ring and linear geometries. Output measurements showed that the devices had excellent electrical and optical properties. Thus, allowing for the larger size of the laser structures, their performance indicates that the etching results in high quality electronic structures.

G. Nanoscale Mapping of Etched Surfaces

As described above, we have carried out extensive work to assess processing damage in III-V materials using photoluminescence. The photoluminescence excitation, which is focused on a circle of 20 μm diameter, encompasses an array of quantum boxes, and is therefore an average response. It does not probe differences in luminescence efficiency and spectral shape between individual quantum boxes or within a single box. Cathodoluminescence, on the other hand, can probe the radiative response of the sample on a much finer, i.e. nano-scale. This additional feature of the cathodoluminescence probe, by virtue of its spatial resolution, gives us an additional handle for understanding sidewall damage in etched structures.

We have established a collaboration with Professor Slade Cargill of the Materials Science Department at Columbia to carry out cathodoluminescence studies of the same samples used in our photoluminescence work. Preliminary work to determine the response to the cathodoluminescence excitation in scan and spot modes has already shown that we can obtain good signal-to-noise ratios from our etched samples for a variety of features. At present, work is centered on the samples prepared by magnetron-induced etching.

Figure 31 shows the cathodoluminescence and corresponding SEM images of two samples

etched at 200 W rf power (30V Bias) and 400 W rf power (75 V Bias), respectively. The latter sample, which exhibits less damage in our photoluminescence experiments, shows a much more uniform and intense cathodoluminescence response. The sample etched at lower bias exhibits a marked nonuniformity in its response. Moreover, the rounded shape of the cathodoluminescence image shows reduced radiative recombination near the corners.

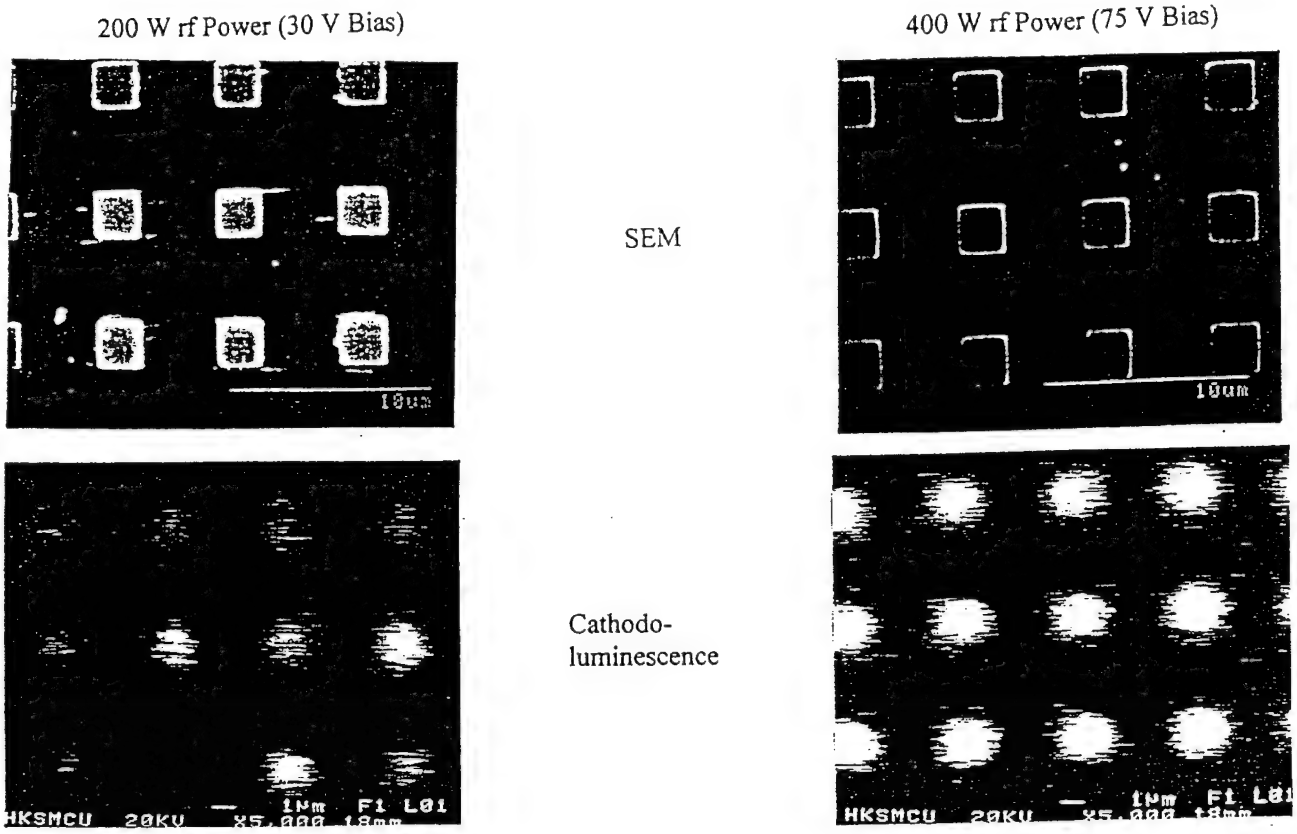

Fig. 31: Bias-voltage tuning to eliminate damage to GaAs/AlGaAs quantum boxes (0.2 μm etch depth). Samples taken from the collaboration with G. McLane of ARL and S. Cargill of Columbia. In the left panel it is seen that the voltage conditions are such that damage is pronounced. It is eliminated in the right panel samples.

By studying the cathodoluminescence response in spot mode, we should be able to map variations in radiative recombination intensity across the etched features, near and away from the sidewalls. This is a crucial study for our nanoscale program since it will allow us to understand how

processing effects the microstructure of small features and, hence, the presence and effect of sidewall damage and non-radiative recombination in our etched structures. We are currently in the midst of extensive studies of these effects.

V. Collaborations and Technology Transfer to Industry and Other Government Programs

A major thrust of this program is to make the results of our research available to industry and other government programs and, where possible, to interact in specific R&D areas. In the space below we summarize our activities in this regard.

A. Selective Processing for Quantum Devices

Our collaboration with the Army Research Laboratory (ARL) at Fort Monmouth over the past year has allowed us to investigate alternate surface making materials and measure the effects of magnetron-enhanced reactive ion etching (MIE) on quantum box performance. In the first aspect of this collaboration, it was found that a Ni surface mask patterned at ARL performed better than the Au/Cr masks typically used in our etching. In the other aspect of this collaboration, MIE was used as a step in the fabrication of quantum boxes. It was found that MIE could be used to fabricate quantum boxes with good luminescence efficiency, and that the etch-induced sidewall damage could be controlled by adjusting the sample bias.

B. Integrated Optics and Photonic Structures

1) Thin film isolator - Collaboration with AT&T Bell Labs. The development of a low cost

isolator is a major requirement in reducing the cost of fiber optic systems.

2) Channel-dropping filter - This was developed through a collaborative effort with Bellcore.

3) Simulation Package - The development of this software package has enabled close collaboration with AlliedSignal, Inc. to aid in the design of low-cost, highly multimode waveguide devices. In the last year, we have emphasized the design of star-coupler devices. The software is currently being packaged and prepared for transfer to industry; we intend to identify a company in the next few months.

4) Via etching technology - Earlier we described the transfer of this technology to Hughes, Malibu. Their interest has been in developing a technique for etching high aspect ratio through wafer vias for use in high speed microwave circuits.

VI. Interactions with DoD Technology

Interactions of Professor Osgood and his group with DOD related technical efforts included: (A) Professor Osgood serves on the steering committee of the ARPA Defense Sciences Research Council, where he served as a major organizer of a Workshop on Optical Lithography (a comparative analysis of advanced optical techniques for UV lithography) and a Workshop on Manufacturing of Critical Optoelectronics; (B) extensive discussions with Antonio Sanchez and Dick Williamson at MIT Lincoln Laboratory on integrated optic and laser applications; (C) collaboration with Dr. Ken Jones and his group at Fort Monmouth on low damage advanced etching technology for ultra small devices; (D) extensive and continuing DoD-sponsored technical interactions with Erich Ippen, Cliff Fonstad, Bill Steier, and Herman Haus at MIT and USC on solid-state physics, laser-surface interactions, and integrated optics; and (E) Prof. Osgood serves on the Advisory Board for LANL

Division on Chemical Science and Technology. This Division at Los Alamos has several significant ARDEC and other DoD Programs.

Appendix A: Publications

1. M. Levy, L. Eldada, R. Scarmozzino, and R. M. Osgood, Jr., "Fabrication of Narrow-Band Channel-Dropping Filters," IEEE Photon. Technol. Lett. **4**, 1378 (1992).

2. T. Fink and R.M. Osgood, Jr., "Photoelectrochemical Etching of GaAs/AlGaAs Multilayer Structures," J. Electrochem. Soc. **140**, 2572 (1993).

3. M. Levy, I. Ilić, R. Scarmozzino, and R. M. Osgood, Jr., "Thin-Film-Magnet Magneto-Optic Waveguide Isolator," IEEE Photon. Technol. Lett. **5**, 198 (1993).

4. T. Fink and R.M. Osgood, Jr., "Light-Induced Selective Etching of GaAs in AlGaAs/GaAs Heterostructures," J. Electrochem. Soc. **140**, L73 (1993).

5. O. Ghandour, R. Scarmozzino and R.M. Osgood, Jr., "Laser-Assisted InP Via Etching for Microwave Device Applications," IEEE Transactions on Semicon. Mftng. **6**, 357 (1993).

6. L. Eldada, M.N. Ruberto, R. Scarmozzino, M. Levy, and R.M. Osgood, Jr., "Laser-Fabricated Low-Loss Single-Mode Waveguiding Devices in GaAs," **10**, 1610 (1993).

7. J. S. Shor and R.M. Osgood, Jr., "Broad Area Photoelectrochemical Etching of n-type B-SiC," J. Electrochem. Soc. **140**, L123 (1993).

8. M.B. Freiler, M. C. Shih, R. Scarmozzino and R.M. Osgood Jr., "Excimer Laser Induced Cryoetching of GaAs and Related Materials," Mat. Res. Soc. Symp. Proc. **279**, 843-848 (1993).

9. A. Villeneuve, C. C. Yang, G. I. Stegeman, C. N. Ironside, G. Scelsi and R.M. Osgood, Jr., "Nonlinear Absorption in a GaAs Waveguide just above half the band gap," IEEE J. Quantum Electron. **30**, 1172 (1993).

10. L. Eldada, N. Zhu, M. Ruberto, M. Levy, R. Scarmozzino and R.M. Osgood, Jr., "Rapid Direct Fabrication of Active Electro-Optic Modulators in GaAs," J. Lightwave Tech. **12**, 1588 (1994).

11. M. Levy, R. Scarmozzino, R.M. Osgood, Jr., R. Wolfe, F.J. Cadieu and H. Hegde, "Permanent Magnet Film Magneto-optic Waveguide Isolator," J. Appl. Phys. **75**, 6286

(1994).

12. I. Ilic, R. Scarmozzino and R. M. Osgood Jr., "Modelling Multimode-Input Star Couplers in Polymers," J. Lightwave Tech. **12**, 996 (1994).

13. L. Eldada, M. Levy, R. Scarmozzino and R. M. Osgood Jr., "Laser Rapid Prototyping of Photonic Integrated Circuits," Proceedings of International Symposium on Integrated Optics **1994**, 2213, (1994).

14. L. Eldada, R. Scarmozzino, R. M. Osgood Jr., D. C. Scott, Y. Chang and H. R. Fetterman, "Laser-Fabricated Delay Lines in GaAs for Optically-Steered Phased-Array Radar," J. Lightwave Tech. (1995).

15. M. C. Shih, M. B. Freiler, R. Scarmozzino and R. M. Osgood Jr., "Patterned, Photon-Driven Cryoetching of GaAs and AlGaAs," J. Vac. Sci. Technol. B **13**, 1 (1995).

16. M. C. Shih, M. Hu, M. B. Freiler, M. Levy, R. Scarmozzino, R. M. Osgood, Jr., I. W. Tao, and W. I. Wang, "Fabrication of an InGaAs SQW Circular Ring Laser by Direct Laser Patterning," Appl. Phys. Lett. **66**, 2608 (1995).

17. J.-L. Lin, M.B. Freiler, M. Levy, D. Collins, T.C. McGill, and R.M. Osgood, Jr., "Photon-Assisted Cryoetching of III-V Binary Compounds by Cl_2 at 193 nm," submitted to Appl. Phys. Lett. (July 1995).

18. M. B. Freiler, G. F. McLane, S. Kim, M. Levy, R. Scarmozzino, R. M. Osgood, Jr., and I. P. Herman, "Luminescence Properties of Submicrometer Scale Features Fabricated Using Magnetron Reactive Ion Etching with Different Sample Biases," submitted to Appl. Phys. Lett. (August, 1995).

19. M. B. Freiler, M. C. Shih, S. Kim, M. Levy, I. P. Herman, R. Scarmozzino, and R. M. Osgood Jr., "Pattern Transfer and Photoluminescence Damage-Assessment of Deep-Submicrometer Features Etched by Laser Cryoetching," submitted to Appl. Phys. Lett. (September, 1995).

Appendix B: Presentations

1. GORDON CONFERENCE, New Hampshire, August 10-14, 1992, Z. Lu and R.M. Osgood, Jr., "*In Situ* Surface Oxidation, Cleaning and Passivation of GaAs and GaSb using a Microwave Electron-Cyclotron-Resonance (ECR) Plasma Source."

2. GORDON RESEARCH CONFERENCE, Meriden, NH, July 27-31, 1992, M.B. Freiler, M.C. Shih, R. Scarmozzino and R.M. Osgood, Jr., "Excimer Laser Driven Cryoetching of GaAs and Related Compounds."

3. UNIVERSITY OF CALIFORNIA AT SANTA BARBARA, September 16, 1992, T. Fink and R.M. Osgood, Jr., "Photoelectrochemical Etching of GaAs/AlGaAs Multilayer Structures."

4. AVS SYMPOSIUM, Chicago, IL, November 9-13, 1992, M.C. Shih, M.B. Freiler, R. Scarmozzino and R.M. Osgood, Jr., "Cryogenic Etching of GaAs Activated by Excimer Laser Radiation of Physisorbed Chlorine."

5. MATS. RES. SOC. SYMP., FALL MEETING, Boston, MA, November 30-December 4, 1992, M.B. Freiler, M.C. Shih, R. Scarmozzino and R.M. Osgood, Jr., "Excimer Laser Induced Cryoetching of GaAs and Related Materials."

6. OPTICAL FIBER CONFERENCE, OFC '93, San Jose, CA, February, 1993, M. Levy, L. Eldada, R. Scarmozzino and R.M. Osgood, Jr., "Fabrication of Narrow-Band Channel-Dropping Filters."

7. OSA SOUTHWESTERN CONNECTICUT CHAPTER, OPTICAL SOCIETY OF AMERICA, Stamford, CT, March 17, 1993, R. Scarmozzino, "Prototyping Integrated Optical Systems."

8. OPTICAL DESIGN FOR PHOTONICS, OPTICAL SOCIETY OF AMERICA, Palm Springs, CA, March 21, 1993, Robert Scarmozzino, "Simulation of Highly Multimode Star Couplers in Polymers."

9. INTEGRATED PHOTONICS RESEARCH (IPR '93) IEEE/OSA MEETING, Palm Springs, CA, March 22-24, 1993, M. Levy, "Sub-Angstrom Planar Channel Dropping Filters."

10. INTEGRATED PHOTONICS RESEARCH (IPR '93), IEEE/OSA MEETING, Palm Springs, CA, March 22-24, 1993, M. Levy, "Compact Thin-Film Waveguide Isolator."

11. NINTH ANNUAL SARNOFF SYMPOSIUM, IEEE/LEOS, Princeton, NJ, March 26, 1993, Osman Ghandour, "Laser-Assisted InP Via Etching for Microwave Device and Circuit Applications."

12. 13TH GENERAL CONFERENCE OF THE CONDENSED MATTER DIVISION, European Physical Society, Regensburg, Germany, March 30, 1993, T. Fink, "Light-Induced Selective Etching of GaAs in AlGaAs/GaAs Heterostructures."

13. CLEO '93, Optical Society of America, Baltimore, MD, May 3, 1993, R. Scarmozzino, "Fabrication of Narrow-Band Channel-Dropping Filters."

14. OPTICAL SOCIETY OF AMERICA, CLEO '93, Baltimore, MD, May 3, 1993, Louay Eldada, "Thin-Film-Magnet-Magneto-Optic Waveguide Isolator."

15. 37TH INT'L. SYMPOSIUM ON ELECTRON, ION AND PHOTON BEAMS, (EIPB '93) San Diego, CA, June 1, 1993, L.H. Hackett, P.D. Brewer, J.L. Visher, O.A. Ghandour, R. Scarmozzino, and R.M. Osgood, Jr. "Via Formation and Metallization of InP Substrates by Laser-Assisted Processes."

16. 37TH INTERNATIONAL SYMPOSIUM ON ELECTRON, ION AND PHOTON BEAMS, AVS, IEEE and OSA, San Diego, CA, July 1, 1993, Osman A. Ghandour, "Via Formation and Metallization of InP Substrates by Laser- Assisted Processes."

17. HYBRID OPTOELECTRONIC INTEGRATION AND PACKAGING, IEEE LEOS Summer Topicals '93, Santa Barbara, CA, July 26-28, 1993, R. Scarmozzino, "Rapid Prototyping of Photonic Integrated Circuits."

18. ILS-IX 9TH INTERDISCIPLINARY LASER SCIENCE CONFERENCE, (OSA '93), Optical Society of America, Toronto, Canada, October 3 - 8, 1993, L. Eldada, N. Zhu, M. Ruberto, M. Levy, R. Scarmozzino, and R.M. Osgood, Jr., "Optimized Polarization Design of GaAs Electro-optic Modulators Using Laser Rapid Prototyping."

19. THIRD INTERNATIONAL SYMPOSIUM ON CLEANING TECHNOLOGY IN SEMICONDUCTOR DEVICE MANUFACTURING, The Electrochemical Society, New Orleans, Louisiana, October 10-15, 1993, Z. Lu, "The Interaction of Hydrogen Plasma with Ga-based III-V Semiconductor Surfaces."

20. OSA ANNUAL MEETING, Toronto, Canada, October 15-19, 1993, I. Ilic, "Design of a Novel, Multimode Input Polymeric Star Coupler for Multi- Wavelength Optical Networks."

21. 38TH ANNUAL CONFERENCE ON MAGNETISM AND MAGNETIC MATERIALS, Minneapolis, MN, November 15, 1993, M. Levy, "Permanent Magnet Film Magneto-optic Waveguide Isolator."

22. 1993 AMERICAN VACUUM SOCIETY MEETING, Orlando, Florida, November, 1993, M.C. Shih, M.B. Freiler, S. Kim, R. Scarmozzino, R.M. Osgood, Jr., and I.P. Herman, "Assessment of Damage Due to Low Temperature, Excimer Laser Induced Etching of GaAs."

23. OSA 1994 INTEGRATED PHOTONICS RESEARCH CONFERENCE, San Francisco, California, February 17-19, 1994. "Beam Propagation and Ray Tracing Simulations of an 8x8 Multimode-Input Star Coupler," I. Ilic, R. Scarmozzino and R. M. Osgood, Jr.

24. PRINCETON UNIVERSITY, Princeton, New Jersey, April 1994. "Photonic Integrated Circuits: Devices, Design and Fabrication," R.M. Osgood, Jr.

25. MASSACHUSSETS INSTITUTE OF TECHNOLOGY, Cambridge, Massachusetts, May 1994. "Photonic Integrated Circuits: Devices, Design and Fabrication," R.M. Osgood, Jr.

26. IEEE/LEOS TOPICAL MEETING ON INTEGRATED OPTICS, Lake Tahoe, NV, July 1994. "Comparative Study of Highly Multimode-Input star Coupler Design Using Beam Propagation and Ray Tracing Simulations," I. Ilic, R. Scarmozzino and R. M. Osgood, Jr.

27. MIT OPTICS COLLOQUIUM, Cambridge, Massachusetts, September 1994. "Design of Photonic Circuits," R.M. Osgood, Jr.

28. 41ST NATIONAL SYMPOSIUM OF THE AMERICAN VACUUM SOCIETY AND NANO 3: Third International Conference on Nanometer-scale Science and Technology, Denver, Colorado, October 24-28, 1994. "Low Damage Surface Cleaning of CdTe by Hydrogen ECR Plasma," Y. Luo, P. J. Lasky, M. C. Shih and R. M. Osgood, Jr.

29. 41ST NATIONAL SYMPOSIUM OF THE AMERICAN VACUUM SOCIETY AND NANO 3: Third International Conference on Nanometer-scale Science and Technology, Denver, Colorado, October 24-28, 1994. "Surface Passivation of Etch-Defined Quantum Structures," M. B. Freiler, M. C. Shih, S. Kim, M. Levy, R. Scarmozzino, I. P. Herman and R. M. Osgood, Jr.

30. 41ST NATIONAL SYMPOSIUM OF THE AMERICAN VACUUM SOCIETY AND NANO 3: Third International Conference on Nanometer-scale Science and Technology, Denver, Colorado, October 24-28, 1994. "Fabrication of Strongly Luminescent Quantum Structures by Neutral-Atom Etching at Cryogenic Temperatures," M. B. Freiler, M. Levy, S. Kim, M. C. Shih, I. P. Herman, R. Scarmozzino and R. M. Osgood, Jr.

31. ARPA/OSA FALL MEETING, Dallas, Texas, Fall 1994. "Photonic-Integrated Optical-Delay Circuit for Phased-Array Radars," L. Eldada, I. Ilic, R. Scarmozzino, R. M. Osgood, Jr. and H. Fetterman.

32. ARPA/OSA FALL MEETING, Dallas, Texas, Fall 1994. "Examination of Wide-Angle Beam Propagation Methods for Accurate Analysis of Waveguiding Circuits," I. Ilic, R. Scarmozzino and R. M. Osgood, Jr.

33. ARPA/OSA FALL MEETING, Dallas, Texas, Fall 1994. "Single-Mode Narrow-Band Channel-Dropping Filter," D. Levy, M. H. Hu, M. Levy, R. Scarmozzino and R. M. Osgood, Jr.

34. MRS 1994 FALL MEETING, Boston, Massachusetts, November 30, 1994. "Beam-Assisted Semiconductor Etching: A Basic Science Approach to Monolayer Control," R. M. Osgood, Jr.

35. POINT PROGRAM INDUSTRIAL MEETING, General Electric R&D Center, Schenectady, New York, December 5, 1994. "Design and Simulation of Optical Interconnects," R. Scarmozzino.

36. SUNY ALBANY PHYSICS COLLOQUIUM, December 9, 1994. "Rapid Prototyping of Photonic Integrated Circuits," M. Levy.

37. TUFTS UNIVERSITY OPTICS COLLOQUIUM, Medford, Massachusetts, December 16, 1994. "Design of Photonic Circuits," R.M. Osgood, Jr.

38. OSA TOPICAL MEETING, INTEGRATED PHOTONICS RESEARCH, Dana Point, CA, February 23, 1995, "Wide-angle Beam Propagation Modeling of Variable-angle Photonic Circuits," I. Ilic, R. Scarmozzino, R.M. Osgood, Jr.

39. MIT ELECTRONIC MATERIALS SEMINAR, Cambridge, MA, March 16, 1995, "Advanced Etching Technologies for Integrated Optics and Quantum-Confined Structures," R.M. Osgood, Jr.

Appendix C: Professional Personnel Associated with this Contract

Principal Investigator
Dr. Richard M. Osgood, Jr., Higgins Professor

Senior Research Scientist
Dr. Robert Scarmozzino

Research Scientist
Dr. Miguel Levy

Associate Research Scientist
Dr. Jong-Liang Lin

Current Graduate Research Assistants
David Levy
Johnny Huang
Martin Hu
Igor Ilic

Former Graduate Research Assistants
Dr. Louay Eldada, awarded the Ph.D. in Electrical Engineering (1994)
Thesis title: "Laser-Controlled Rapid Prototyping of Photonic Integrated Circuits"

Dr. Michael Freiler, awarded the Ph.D. in Electrical Engineering (1995)
Thesis title: "The Application of Photon-Driven Cryoetching to Micro- and Nanostructure Fabrication"

Dr. Osman A. Ghandour, awarded the Ph.D. in Electrical Engineering (1994)
Thesis title: "Laser-Assisted Indium Phosphide Via Etching for Applications in Microwave, Millimeter-Wave, Optical and Optoelectronic Integrated Circuits"

Dr. Ming Chang Shih, awarded the Ph.D. in Electrical Engineering (1994)
Thesis title: "Characterization of Low Temperature Photochemical Etching of GaAs and its Application"